

The linear polarization of Southern bright stars measured at the parts-per-million level

Daniel V. Cotton,^{1,2★} Jeremy Bailey,^{1,2} Lucyna Kedziora-Chudczer,^{1,2}
Kimberly Bott,^{1,2} P. W. Lucas,³ J. H. Hough³ and Jonathan P. Marshall^{1,2}

¹*School of Physics, UNSW Australia, NSW 2052, Australia*

²*Australian Centre for Astrobiology, UNSW Australia, NSW 2052, Australia*

³*Centre for Astrophysics Research, Science & Technology Research Institute, University of Hertfordshire, Hatfield AL10 9AB, UK*

Accepted 2015 September 18. Received 2015 September 18; in original form 2015 August 19

ABSTRACT

We report observations of the linear polarization of a sample of 50 nearby Southern bright stars measured to a median sensitivity of $\sim 4.4 \times 10^{-6}$. We find larger polarizations and more highly polarized stars than in the previous PlanetPol survey of Northern bright stars. This is attributed to a dustier interstellar medium in the mid-plane of the Galaxy, together with a population containing more B-type stars leading to more intrinsically polarized stars, as well as using a wavelength more sensitive to intrinsic polarization in late-type giants. Significant polarization had been identified for only six stars in the survey group previously, whereas we are now able to deduce intrinsic polarigenic mechanisms for more than 20. The four most highly polarized stars in the sample are the four classical Be stars (α Eri, α Col, η Cen and α Ara). For the three of these objects resolved by interferometry, the position angles are consistent with the orientation of the circumstellar disc determined. We find significant intrinsic polarization in most B stars in the sample; amongst these are a number of close binaries and an unusual binary debris disc system. However, these circumstances do not account for the high polarizations of all the B stars in the sample and other polarigenic mechanisms are explored. Intrinsic polarization is also apparent in several late-type giants which can be attributed to either close, hot circumstellar dust or bright spots in the photosphere of these stars. Aside from a handful of notable debris disc systems, the majority of A–K type stars show polarization levels consistent with interstellar polarization.

Key words: polarization – techniques: polarimetric – binaries: close – stars: emission-line, Be – stars: late-type – ISM: magnetic fields.

1 INTRODUCTION

The measured linear polarization of starlight falls into two categories: it is either intrinsic to the star and its immediate environment (i.e. the star system), or it is interstellar in origin. Interstellar polarization is the result of interstellar dust particles aligning with the Galactic magnetic field. Studies of this polarization reveal details of the dust distribution and the Galactic magnetic field structure (Heiles 1996) as well as the size and nature of the dust particles (Whittet et al. 1992; Kim, Martin & Hendry 1994). Linear polarimetry is therefore a powerful technique for investigating the interstellar medium.

Linear polarization measurements of stars have, until fairly recently, been limited to sensitivities in fractional polarization of

$\sim 10^{-4}$. At this level most nearby ($d < 100$ pc) stars are found to be unpolarized (Tinbergen 1982; Leroy 1993a,b, 1999). A new generation of high-precision polarimeters has recently been developed that allow polarization measurements of starlight at the parts per million level (Hough et al. 2006; Wiktorowicz & Matthews 2008; Bailey et al. 2015; Wiktorowicz & Nofi 2015). With such instruments, it is possible to detect significant interstellar polarization even in nearby stars. Bailey, Lucas & Hough (2010) reported such a survey of 49 bright nearby Northern hemisphere stars (the PlanetPol survey) and found that the majority of stars show significant polarization, in most cases consistent with an interstellar origin.

In this paper, we present the first survey of the polarization of Southern bright nearby stars measured at the parts per million level. The survey utilized the newly commissioned HIPPI (HIgh Precision Polarimetric Instrument; Bailey et al. 2015) to observe 50 of the brightest Southern stars within 100 pc. The observing methods are described in detail in Section 2. In contrast to the PlanetPol survey

*E-mail: d.cotton@unsw.edu.au

(Bailey et al. 2010) described above, the Southern sample reported here contains many stars that are intrinsically polarized.

Intrinsic polarization is well known to be present in Be stars as a result of scattering from a transient gaseous circumstellar disc and our sample includes four classical Be stars. These are indeed the four highest polarizations measured. However, compared to other stars we observed we also find higher than average polarizations in several B stars, not known to be Be stars. These results are discussed in Sections 4.8 and 4.9, respectively. Other sources of intrinsic polarization found in the sample are the presence of a debris disc around the star (Section 4.4), and polarization, probably mostly due to dust scattering, in late-type giants (Section 4.10).

Another area of interest is the level to which normal stars are intrinsically polarized. The quiet Sun has been directly measured, and shows polarization of $<3 \times 10^{-7}$ (Kemp et al. 1987). Star-spots in active stars will show higher polarization (Strassmeier 2009; Wiktorowicz 2009). As well as being interesting in their own right, star-spots can complicate the growing and exciting field of exoplanet polarimetry (Wiktorowicz 2009).

Polarimetry can be used to detect unresolved hot-Jupiter type planets (Seager, Whitney & Sasselov 2000; Lucas, Hough & Bailey 2006; Lucas et al. 2009), as a differential technique to detect planets in imaging (Schmid et al. 2005; Keller 2006) or transit observations (Kostogryz, Berdyugina & Yakobchuk 2015), and to characterize exoplanet atmospheres (Bailey 2007; Kopparla, Natraj & Yung 2014). In each of these applications, the signal from the planet is small. The effectiveness of the technique will depend upon an understanding of non-planetary sources of polarization as much as planetary ones. For this reason, an investigation and characterization of the primary sources of stellar linear polarization is important.

2 OBSERVATIONS

2.1 The sample stars

Stars selected for observation were south of the equator, were at a distance of less than 100 pc^1 , and have V magnitude brighter than 3.0^2 . 54 stars met these criteria and we have observed 50 of them. The stars observed are listed in Table 1. This table gives the V magnitude and spectral type as listed in the SIMBAD (Wenger et al. 2000) database³, the distance derived from the *Hipparcos* catalogue parallax (Perryman et al. 1997; van Leeuwen 2007), the Galactic co-ordinates (also from the *Hipparcos* catalogue), and rotational velocity ($V \sin i$) from a variety of sources as indicated in Table 1. Where a distinction has been made in the reference, the value given is for the primary in multiple systems. The number of companions that fall within the aperture was determined in the first instance from Burnham’s *Celestial Handbook* (Burnham 1978a,b,c)

¹ One star, HIP 89931, has a distance greater than 100 pc as a result of revision of its parallax after the sample was selected.

² A V magnitude of 3.0 corresponds to an absolute magnitude of -2.0 at 100 pc .

³ HIP 60718, has no listed luminosity class in SIMBAD, and so instead we use the spectral type given by Bartkevicius & Gudas (2001). There are a number of multiple systems listed, HIP 93506 and HIP 65474, for example, are both noteworthy double star systems where both stars are of B spectral type, where the combined spectral type is given by SIMBAD this is what is given in Table 1. If a companion also falls within the HIPPI aperture this is marked with an ‘*’ in the succeeding column.

and from Eggleton & Tokovinin (2008), then followed up with a variety of sources as indicated in the footnote of Table 1.

Previous polarization measurements for the stars are listed in Table 2 and have been taken from the agglomerated polarization catalogue of Heiles (2000). Only the degree of polarization is listed. The position angle can be found in the original catalogue, but for almost all the measurements the polarization is not significant and the position angle is therefore meaningless. The only stars with significant polarizations in this catalogue are the four Be stars, which will be discussed later, the SRB (semi-regular) type pulsating variable HIP 112122 (β Gru) which has a listed polarization angle of $155:2 \pm 4.6$, and possibly the short period binary and variable of the β Cep type HIP 65474 (Spica) with a listed polarization angle of $147:0 \pm 0.0$.

The Heiles (2000) catalogue does not include the slightly more accurate previous polarization measurements of nearby stars made by Tinbergen (1982). This study includes a number of the stars in our sample and is therefore listed separately in Table 2. The measurements of Tinbergen were made in three colour bands. We have tabulated the averaged band I and II measurements. Of the stars observed by Tinbergen (1982) only HIP 89931 (δ Sgr) and Spica have a significant polarization.

In addition to the measurement listed in Table 2, it might be noted that Sirius (HIP 32349) also has a reported measurement in Bailey et al. (2015) where it was used as a low polarization standard to determine telescope polarization (TP). When the TP is subtracted the polarization of Sirius is $3 \pm 4 \text{ ppm}$.

2.2 Observation methods

The observations were obtained with the HIPPI polarimeter (Bailey et al. 2015) over the course of four observing runs (2014 May 8–12, 2014 August 28–September 2, 2015 May 21–26 and 2015 June 25–29) at the 3.9 m Anglo Australian Telescope (AAT). The AAT is located at Siding Spring Observatory near Coonabarabran in New South Wales, Australia. HIPPI was mounted at the $f/8$ Cassegrain focus of the telescope where it had an aperture size of 6.7 arcsec . The seeing varied between $\sim 1.5 \text{ arcsec}$ and $>4 \text{ arcsec}$ with a typical seeing around $2\text{--}2.5 \text{ arcsec}$.

HIPPI is a high-precision polarimeter, with a sensitivity in fractional polarization of $\sim 4.3 \times 10^{-6}$ on stars of low polarization and a precision of better than 0.01 percent on highly polarized stars (Bailey et al. 2015). It achieves this by the use of a Ferroelectric Liquid Crystal (FLC) modulator operating at a frequency of 500 Hz to eliminate the effects of variability in the atmosphere. From the modulator the light passes through a Wollaston prism that acts as a beam splitter, directing the light into two Photo Multiplier Tube (PMT) detectors. Second stage chopping, to reduce systematic effects, is accomplished by rotating the entire back half of the instrument after the filter wheel through 90° in an ABBA pattern, with a frequency of once per 40 s. An observation of this type measures only one Stokes parameter of linear polarization. To get the orthogonal Stokes parameter, the entire instrument is rotated through 45° and the sequence repeated. The rotation is performed using the AAT’s Cassegrain instrument rotator. In practice, we also repeat the observations at telescope position angles of 90° and 135° to allow removal of instrumental polarization. The stars in the survey were observed for a total integration time of 12 min in each (Q and U) Stokes parameter per observation. This gave a median sensitivity in fractional polarization of $\sim 4.4 \times 10^{-6}$. The observing, calibration and data reduction methods are described in full detail in Bailey et al. (2015).

Table 1. Properties of survey stars.

HIP	BS	Other names	V mag	Spectral type	Comp in Ap ^a	Dist (pc)	RA (hh mm)	Dec. (dd mm)	Galactic Long	Galactic Lat	V sin <i>i</i> (km/s)	$F_{\text{IR}}/F_{\star}^b$ ($\times 10^{-6}$)
2021	98	β Hya	2.79	G0V		7.5	00 26	-77 15	304.77	-39.78	$4.1 \pm 1.0^{\text{dM}}$	
2081	99	α Phe	2.37	K0.5IIIb		25.9	00 26	-42 18	320.00	-73.98	$< 1.2^{\text{dM}}$	
3419	188	β Cet	2.01	K0III		29.5	00 44	-17 59	111.33	-80.68	$3.6 \pm 1.0^{\text{dM}}$	
7588	472	α Eri, Achernar	0.46	B6Vep		42.9	01 38	-57 14	290.84	-58.79	$207 \pm 9^{\text{Y}}$	0.027
9236	591	α Hya	2.84	F0IV		22.0	01 59	-61 34	289.44	-53.76	$118 \pm 12^{\text{ZR}}$	34.24
13847	897	θ Eri	2.90	A4III		49.4	02 58	-40 18	247.86	-60.74	$70 \pm 17^{\text{R}}$	
18543	1231	γ Eri	2.94	M1IIIb		62.3	03 58	-13 30	205.16	-44.47	$3.8 \pm 0.3^{\text{M}}$	
26634	1956	α Col	2.65	B9Ve		80.1	05 40	-34 04	238.81	-28.86	$184 \pm 5^{\text{Y}}$	1.484
30438	2326	α Car, Canopus	-0.74	A9II		94.8	06 24	-52 42	261.21	-25.29	$9.0 \pm 1.0^{\text{R}}$	0.033
32349	2491	α CMa, Sirius	-1.46	A1V		2.6	06 45	-16 43	227.23	-08.89	$16 \pm 1^{\text{R}}$	
39757	3185	ρ Pup	2.81	F5II		19.5	08 08	-14 18	243.15	04.40	$15 \pm 1^{\text{GG}}$	160.7
42913	3485	δ Vel	1.95	A1Va(n)	*	24.7	08 45	-54 43	272.08	-07.37	$150 \pm 15^{\text{ZR}}$	4.567
45238	3685	β Car	1.69	A1III		34.7	09 13	-69 43	285.98	-14.41	$146 \pm 2^{\text{D}}$	6.700
46390	3748	α Hya, Alphard	1.97	K3II-III		54.0	09 28	-08 40	241.49	29.05	$< 1.0^{\text{dM}}$	3.359
52727	4216	μ Vel	2.69	G6III	*	35.9	10 47	-49 25	283.03	08.57	$6.4 \pm 1.0^{\text{dMM}}$	19.94
59803	4662	γ Crv	2.58	B8III		47.1	12 16	-17 33	290.98	44.50	$30 \pm 9^{\text{A}}$	
60718		α Cru	0.81	B0.5IV	* ^c	98.7	12 27	-63 06	300.13	-00.36	$88 \pm 5^{\text{GG}}$	0.001
60965	4757	δ Crv	2.94	A0IV(n)		26.6	12 30	-16 31	295.47	46.04	$236 \pm 24^{\text{ZR}}$	
61084	4763	γ Cru	1.64	M3.5III		27.2	12 31	-57 07	300.17	05.65	$4.7 \pm 0.9^{\text{C}}$	
61359	4786	β Crv	2.64	G5II		44.7	12 34	-23 24	297.87	39.31	$4.2 \pm 1.0^{\text{dMM}}$	5.154
61585	4798	α Mus	2.68	B2IV-V		96.7	12 37	-69 08	301.66	-06.30	$114 \pm 11^{\text{W}}$	0.179
61932	4819	γ Cen	2.17	A1IV+A0IV	*	39.9	12 42	-48 58	301.25	13.88	$79 \pm 3^{\text{GG}}$	
61941		γ Vir	2.74	F0IV+F0IV	*	11.7	12 42	-01 27	297.83	61.33	$36 \pm 4^{\text{ZR}}$	
64962	5020	γ Hya	3.00	G8III		41.0	13 19	-23 10	311.10	39.26	$3.7 \pm 1.0^{\text{dM}}$	2.931
65109	5028	ι Cen	2.73	A2V		18.0	13 20	-36 43	309.41	25.79	$90 \pm 2^{\text{D}}$	14
65474	5056	α Vir, Spica	0.97	B1III-IV	*	77.0	13 25	-11 10	316.11	50.84	$140 \pm 6^{\text{GG}}$	0.003
68933	5288	θ Cen	2.05	K0III		18.0	14 07	-36 22	319.45	24.08	1.2^{GG}	
71352	5440	η Cen	2.31	B1.5Vne		93.7	14 36	-42 09	322.77	16.67	$291 \pm 32^{\text{Y}}$	0.443
71683	5459	α Cen	0.10	G2V+K1V	*	1.3	14 40	-60 50	315.73	-00.68	$2.3 \pm 0.5^{\text{We}}$	
72622	5531	α^2 Lib	2.75	A3V	*	23.2	14 50	-16 02	340.32	38.01	$102 \pm 10^{\text{ZR}}$	16.25
74785	5685	β Lib	2.62	B8Vn	*	56.8	15 17	-09 22	352.02	39.23	$250 \pm 24^{\text{A}}$	3.652
74946	5671	γ TrA	2.89	A1V		56.4	15 19	-68 41	315.71	-09.55	$199 \pm 20^{\text{ZR}}$	5.391
77952	5897	β TrA	2.85	F1V		12.4	15 55	-63 26	321.85	-07.52	92^{Ma}	
79593	6056	δ Oph	2.75	M0.5III		52.5	15 14	-03 41	8.84	32.20	$7.0 \pm 0.0^{\text{M}}$	
82396	6241	ϵ Sco	2.29	K1III		19.5	16 50	-34 18	348.81	06.56	$< 1.0^{\text{dM}}$	
84012	6378	η Oph	2.42	A2IV-V	*	27.1	17 10	-15 44	6.72	14.01	$23 \pm 2^{\text{ZR}}$	19.01
85792	6510	α Ara	2.95	B2Vne		82.0	17 32	-49 52	340.75	-08.83	$269 \pm 13^{\text{Y}}$	15.62
86228	6553	θ Sco	1.86	F1III		92.1	17 37	-43 00	347.14	-05.98	125^{vB}	3.023
88635	6746	γ^2 Sgr	2.99	K1III		29.7	18 06	-30 25	0.92	-04.54	$< 1.0^{\text{dM}}$	146.7
89311	6859	δ Sgr	2.71	K3IIIa		106.6	18 21	-29 50	3.00	-70.15	$3.6 \pm 1.0^{\text{dM}}$	1.305
90185	6879	ϵ Sgr	1.85	B9.5III	*	43.9	18 24	-34 23	359.19	-09.81	175^{vB}	31
90496	6913	λ Sgr	2.81	K0IV		24.0	18 28	-25 25	7.66	-06.52	$< 1.1^{\text{dM}}$	
92855	7121	σ Sgr	2.06	B2V		69.8	18 55	-26 18	9.56	-12.43	205^{vB}	0.025
93506	7194	ζ Sgr	2.61	A2.5Va	*	27.0	19 03	-29 53	6.84	-15.35	$77 \pm 8^{\text{ZR}}$	7.111
100751	7790	α Pav	1.91	B2IV	*	54.8	20 26	-56 44	340.9	-35.19	$15 \pm 3^{\text{GG}}$	0.038
107556	8322	δ Cap	2.83	A7III	*	11.9	21 47	-16 08	37.60	-46.01	$93 \pm 10^{\text{GG}}$	
109268	8425	α Gru	1.71	B6V		31.0	22 08	-46 58	349.99	-52.47	$259 \pm 26^{\text{ZR}}$	
110130	8502	α Tuc	2.82	K3III	*	61.3	22 19	-60 16	330.22	-47.96	$1.9 \pm 1.3^{\text{dM}}$	6.579
112122	8636	β Gru	2.11	M5III		54.3	22 43	-46 53	346.27	-57.95	$2.5 \pm 1.5^{\text{Z}}$	
113368	8728	α PsA, Fomalhaut	1.16	A4V		7.7	22 58	-29 37	20.49	-64.91	$93 \pm 9^{\text{ZR}}$	22

Notes. ^aAn asterisks indicates a companion also lies within the aperture. Sources for these determinations are: Burnham (1978a,b,c), Eggleton & Tokovinin (2008), Pourbaix et al. (2004); Spica – Harrington et al. (2009); ϵ Sgr – Hubrig et al. (2001); β Lib – Roberts, Turner & ten Brummelaar (2007).

^bFractional infrared excess from McDonald, Zijlstra & Boyer (2012), except for ι Cen and Fomalhaut (Marshall et al. in preparation), and ϵ Sgr for which we derived the fractional luminosity based on excesses reported by Rhee et al. (2007) and Chen et al. (2014).

^cThere are at least two stars within the aperture, there may be as many as four (see Section 3.1.2).

Rotational velocity references: dM - De Medeiros et al. (2014), Y - Yudin (2001), ZR - Zorec & Royer (2012), R - Royer et al. (2002), M - Massarotti et al. (2008), dMM - de Medeiros & Mayor (1999), A - Abt, Levato & Grosso (2002), GG - Głęboccki & Gnaciński (2005), C - Cummings (1998), W - Wolff et al. (2007), D - Díaz et al. (2011), We - Weise et al. (2010), Ma - Mallik, Parthasarathy & Pati (2003), vB - van Belle (2012), Z - Zamanov et al. (2008).

Table 2. Previous polarization measurements.

HIP	Polarization (Heiles)	Polarization (Tinbergen) ^a	
	p (per cent)	q (ppm)	u (ppm)
2021	0.050 ± 0.035	60 ± 60	0 ± 60
2081	0.011 ± 0.006	60 ± 60	−70 ± 60
3419	0.004 ± 0.005	40 ± 60	−60 ± 60
7588 ^b	0.011 ± 0.002	10 ± 60	−10 ± 60
9236		30 ± 60	−10 ± 60
13847	0.003 ± 0.003		
26634 ^b	0.150 ± 0.100		
32439		0 ± 60	−40 ± 60
46390	0.150 ± 0.120	30 ± 60	10 ± 60
52727		30 ± 60	−40 ± 60
59803	0.050 ± 0.120		
60965	0.030 ± 0.120		
61359		120 ± 60	−30 ± 60
61941	0.030 ± 0.120	60 ± 60	70 ± 60
65109		−30 ± 60	110 ± 60
65474 ^c	0.010 ± 0.000	−220 ± 60	−10 ± 60
		−150 ± 60	−60 ± 60
71352 ^b	0.040 ± 0.100		
71683		−70 ± 60	30 ± 60
74785	0.050 ± 0.120		
77952		−40 ± 60	40 ± 60
79593	0.020 ± 0.120		
82396		60 ± 60	−90 ± 60
84012	0.026 ± 0.004		
85792 ^b	0.610 ± 0.035		
86228	0.030 ± 0.035		
89931		−110 ± 60	−520 ± 60
90496		90 ± 60	−150 ± 60
107556		−40 ± 60	−40 ± 60
109268	0.003 ± 0.005	−70 ± 60	10 ± 60
110130	0.011 ± 0.004		
112122	0.031 ± 0.005		
113368	0.005 ± 0.005	10 ± 60	−110 ± 60

Notes. ^aThe polarizations were originally reported with units of 10^{-5} .

^bClassical Be star.

^cSpica appears in Tinbergen's table twice; observed from Hartebeespoortdam (top) and LaSilla (bottom).

Typically, a sky measurement was acquired at each telescope position angle an object was observed in, and subtracted from the measurement. The duration of the sky measurements was 3 min per Stokes parameter. For particularly bright objects (or those known to be highly polarized) observed under a moonless sky, the sky signal is negligible and a dark measurement was sufficient for calibration purposes. Dark measurements are obtained with the use of a blank in the filter wheel and the instrument otherwise configured identically. Whether a sky subtraction or only a dark subtraction was carried out is indicated in Table 5. These subtractions were carried out as the first step of the data reduction routine.

During the observations at the AAT, zero-point calibration was carried out by reference to the average of a set of observed stars that have been measured as having negligible polarization. This method was used owing to a lack of other available unpolarized standard stars in the Southern hemisphere, and allowed us to determine the TP for the equatorially mounted AAT. Using this method, the polarization of the telescope was determined as $48 \pm 5 \times 10^{-6}$ during the Aug–Sep run (Bailey et al. 2015). This value was used for correction of both 2014 runs, with the uncertainty in the measurement contributing to the stated errors. Shortly before the 2015 May run, the telescope mirror was re-aluminized necessitating a new deter-

Table 3. Low polarization star measurements to determine TP for the 2015 May and June runs in the g' filter. The adopted TP for 2015 June uses all seven measurements, that for 2015 May just those acquired in that month.

Star	Date	p (ppm)	θ (°)
Sirius	23 May	39.2 ± 1.4	91.0 ± 2.1
	24 May	40.2 ± 0.8	89.5 ± 1.1
BS 5854	22 May	30.4 ± 5.1	70.2 ± 9.7
	26 May	37.6 ± 4.0	84.4 ± 6.1
Adopted TP	May 2015	35.5 ± 1.4	84.7 ± 2.3
BS 5854	26 Jun	43.3 ± 4.4	93.4 ± 5.9
	27 Jun	32.9 ± 3.9	70.6 ± 6.8
β Leo	26 Jun	43.6 ± 2.4	87.0 ± 3.2
Adopted TP	Jun 2015	36.5 ± 1.2	84.8 ± 1.4

mination of the TP. This procedure was carried out as before, with the details given in Table 3. HIPPI was left in place at the AAT Cassegrain focus between the 2015 May and June runs. Three additional measurements of low polarization standards (β Leo, and two of BS 5854) were made in June. To increase the precision of the determination for 2015 June, the average of all the May and June measurements was adopted as the TP for that run – this is reasonable given the negligible difference in the determinations. The TP was found to be $36.5 \pm 1.2 \times 10^{-6}$.

A number of stars with known high polarizations (~ 1 –5 per cent) were observed during the Aug–Sep run, and used to help calibrate the modulation efficiency of the telescope as reported by Bailey et al. (2015). The same stars were used to determine the position angle zero-point for the Aug–Sep run, whereas a different set were needed for the other runs; these were HD 147084, HD 154445, HD 160529 and HD 187929 in 2014 May; HD 147084 and HD 154445 in 2015 May; and HD 147084 and HD 154445 in 2015 June. The precision of each determination is less than 1° , based on the consistency of the calibration provided by the different reference stars which themselves have uncertainties of this order.

HIPPI has been tuned to be most sensitive at the blue end of the visible spectrum, in order to investigate polarization induced in exoplanet atmospheres by Rayleigh scattering from clouds (Bailey et al. 2015). It achieved this through the use of PMTs with ultrabialkali photocathodes, giving a quantum efficiency of 43 per cent at 400 nm. HIPPI is equipped with a number of filters. The initial observations reported here were carried out exclusively using the SDSS g' (400–550 nm) filter.

The g' band is centred on 475 nm and is 150 nm in width, which results in the precise effective wavelength⁴ and modulation efficiency changing with star colour. Table 4 gives the effective wavelength and modulation efficiency for various spectral types based on a bandpass model as described in Bailey et al. (2015). It combines the attenuation of the atmosphere, as well as PMT response and other instrumental responses as well as that of the g' filter. No interstellar extinction (i.e. $E(B - V) = 0$) has been applied here. This is reasonable as at 100 pc, the extinction is well below that which can actually be measured by photometry (Bailey et al. 2010). The efficiencies in Table 4 were applied to the raw Q/I and U/I polarizations of each object according to its spectral type given in Table 1 (we apply a linear interpolation between the given types).

⁴ Effective wavelength is the intensity weighted mean of the wavelength of observed photons.

Table 4. Effective wavelength and modulation efficiency for different spectral types according to band-pass model.

Spectral Type	Effective wavelength (nm)	Modulation efficiency (per cent)
B0	459.1	87.7
A0	462.2	88.6
F0	466.2	89.6
G0	470.7	90.6
K0	474.4	91.6
M0	477.5	92.0
M5	477.3	91.7

Follow up observations were made for one object using SDSS r' and 425 nm short pass (425SP) filters on 2015 May 24. The same procedures were used for calibrating TP, angular calibration and efficiency as for the observations made using the SDSS g' band. The r' filter is 150 nm in width; it is centred on 625 nm but HIPPI's PMTs decrease in efficiency steadily from ~ 525 nm, giving a shorter effective wavelength (this is depicted graphically in Bailey et al. 2015). The response of the 425SP filter at the blue end is truncated by the detector response at ~ 350 nm.

2.3 Accounting for patchy cloud

Some of the observations were made in cloudy conditions. For three objects (HIP 88635, HIP 107556 and to a lesser degree HIP 90496), the precision is considerably worse than the median (see Table 5) owing to particularly poor weather on 2014 September 1. Thick, rapidly moving patchy (mostly nimbus) cloud was constant for much of the night, and seeing was worse than 4 arcsec at one point. Similarly patchy cloud also affected observations on September 2nd, but not to the same degree.

To account for this, we removed the most cloud affected parts of the observations. The HIPPI observing technique allows for the efficient flagging and elimination of bad data. The data are taken in lots of 20 one-second integrations per rotation. The Stokes parameters Q or U and I are determined for each integration using a Mueller matrix method (see Bailey et al. 2015 for more details). The errors are then determined based on the number statistics of all the integrations in a rotation. Integrations with a Stokes I determination of less than 5 per cent of the maximum observed for the corresponding Q or U Stokes parameter were discarded as cloud affected. The precision of the measurements is improved by removing the cloud affected integrations. However, each observation was initiated in as clear as possible conditions to ensure an appropriate maximum I .

The 5 per cent threshold was arrived at from very many repeated observations of HIP 2081 on September 1st, producing hundreds of integrations, made during the most varied observing conditions. By examining a moving average of one Stokes parameter with I , it was found that the accuracy of polarization determinations was not affected, only the precision, at least down to a threshold of 3 per cent.

3 RESULTS

The resulting polarization measurements for the 50 stars are given in Table 5. This table lists the normalized Stokes parameters $q = Q/I$ and $u = U/I$, on the equatorial system, and the degree of polarization and position angle obtained by combining the q and u measurements as $p = \sqrt{q^2 + u^2}$. The polarizations and Stokes

parameters are in units of parts per million (ppm, equal to 10^{-6}) in fractional polarization.

The errors quoted are derived from the internal statistics of the individual data points included in each measurement as described in Section 2.3 and by Bailey et al. (2015).

3.1 Uncertain results for binaries with aperture scale separations

The process of centring a star in HIPPI's 6.7 arcsec aperture is carried out by manual scanning to maximize the total signal received by the instrument. This process is made difficult when stars in a binary system have a separation similar to the radius of the aperture, particularly if they have a similar apparent magnitude, or if the seeing is poor. This can result in the system being off-centre in the aperture, and a partial contribution from the secondary. In such instances, a small instrumental polarization is induced that would be difficult to calibrate for.

3.1.1 α Cen

This particular difficulty was apparent when attempting to acquire α Cen A (HIP 71683). The separation of α Cen A (G2V) and B (K1V) at the time of our observations was around 4 arcsec (the separation is depicted graphically by Burnham 1978a, and the updated parameters given by Pourbaix et al. 2002 are little different). We certainly have a significant contribution from component B also, and so we have reported the polarization for the α Cen system as a whole. In the discussion that follows, it will become clear that the degree of polarization of α Cen is anomalously high when one considers its spectral type and proximity to the Sun, and we ascribe this to aperture scale separation of α Cen B inducing instrumental polarization.

3.1.2 α Cru

Although not apparent at the time, it is possible that α Cru (HIP 60718) is affected in the same way. The components α^1 (B0.5IV) and α^2 (B1V) are also separated by ~ 4 arcsec (Burnham 1978b; Pourbaix et al. 2004). α Cru shows higher polarization than any other (non-Be) B type star in our survey which suggests that its measurement is spurious. However, there are other factors that may result in a high degree of polarization for α Cru. It is the star system in the survey with the earliest spectral type, and the α^1 component is itself a binary with a separation of ~ 1 au, while α^2 may also be a binary (Burnham 1978b; Pourbaix et al. 2004). These factors are discussed with reference to other stars in Sections 4.9 and 4.7.

4 DISCUSSION

The discussion begins with a comparison to previous results (Section 4.1) and a look at the statistics of the survey (Section 4.2). Thereafter, it is divided up roughly by stellar spectral type. Porigenic mechanisms for A–K stars begin with the spatial distribution of polarization due to the interstellar medium (Section 4.3), we then look at debris disc systems (Section 4.4), Ap stars (Section 4.5) and eclipsing binaries (Section 4.6). B spectral types are examined next beginning with close binaries (Section 4.7), then Be stars

Table 5. HIPPI linear polarization measurements.

Star	Date(s) ^a	Cal ^b	q (ppm)	u (ppm)	p (ppm)	θ (°)
HIP 2021	28–31/8/14	D	-8.6 ± 2.5	-1.6 ± 2.5	8.8 ± 2.5	95.1 ± 16.3
HIP 2081	1/9/14	S	-5.4 ± 4.6	-82.0 ± 3.9	82.1 ± 4.3	133.1 ± 3.2
HIP 3419	2/9/14	S	-23.1 ± 8.0	-4.1 ± 7.8	23.5 ± 7.9	95.1 ± 19.1
HIP 7588	2/9/14, 24/5/15	D, S	969.6 ± 4.0	1920.9 ± 3.6	2151.8 ± 3.8	31.6 ± 0.1
HIP 9236	2/9/14	D	31.7 ± 8.2	-28.1 ± 8.7	42.4 ± 8.4	159.2 ± 11.5
HIP 13847	2/9/14	D	33.6 ± 8.8	65.9 ± 8.0	74.0 ± 8.4	31.5 ± 6.7
HIP 18543	31/8/14, 2/9/14	D	42.0 ± 6.7	2.9 ± 6.0	42.1 ± 6.3	1.9 ± 8.2
HIP 26634	31/8/14	S	-668.4 ± 6.5	-273.1 ± 6.3	722.0 ± 6.4	101.1 ± 0.5
HIP 30438	28–30/8/14, 2/9/14	D	-68.9 ± 1.7	-89.2 ± 1.6	112.8 ± 1.7	116.2 ± 0.9
HIP 32349 ^c	31/8/14, 2/9/14, 23–24/5/15	D	-3.7 ± 1.7	-4.0 ± 1.7	5.5 ± 1.7	113.8 ± 17.8
HIP 39757	25/5/15	S	-13.4 ± 5.8	-12.5 ± 5.8	18.3 ± 5.8	111.5 ± 18.2
HIP 42913	25/5/15	S	-10.9 ± 8.0	-43.1 ± 8.0	44.5 ± 8.0	127.9 ± 10.4
HIP 45238	23/5/15	S	-20.5 ± 3.3	12.4 ± 3.4	23.9 ± 3.4	74.4 ± 8.1
HIP 46390	24/5/15	S	8.4 ± 4.7	-2.8 ± 4.7	8.8 ± 4.7	170.8 ± 30.3
HIP 52727	12/5/14	S	-12.7 ± 5.3	-30.4 ± 4.6	33.0 ± 4.9	123.7 ± 9.0
HIP 59803	12/5/14	S	9.7 ± 4.3	-68.2 ± 3.4	68.9 ± 3.9	139.1 ± 3.5
HIP 60718	12/5/14, 26/6/15	S	-248.1 ± 2.3	-258.7 ± 1.9	358.4 ± 2.1	113.1 ± 0.3
HIP 60965	24/5/14	S	-14.3 ± 4.8	12.1 ± 4.8	18.7 ± 4.8	70.0 ± 14.7
HIP 61084	12/5/14	S	-19.8 ± 4.2	-39.8 ± 3.5	44.5 ± 3.9	121.8 ± 5.3
HIP 61359	12/5/14	S	-29.1 ± 4.8	15.3 ± 4.1	32.9 ± 4.4	76.1 ± 7.4
HIP 61585	12/5/14	S	145.7 ± 4.7	3.3 ± 3.4	145.7 ± 4.0	0.7 ± 1.3
HIP 61932	24/5/15	S	-37.7 ± 5.3	48.8 ± 5.1	61.6 ± 5.2	63.8 ± 4.9
HIP 61941	24/5/15	S	-5.3 ± 5.0	-5.4 ± 5.1	7.6 ± 5.0	112.5 ± 38.2
HIP 64962	12/5/14	S	2.2 ± 5.1	5.6 ± 4.5	6.1 ± 4.8	34.3 ± 47.9
HIP 65109	2/9/14	S	-25.7 ± 4.9	22.2 ± 4.7	34.0 ± 4.8	69.6 ± 8.0
HIP 65474	24/5/15, 2×29/6/15	S	-200.2 ± 2.0	42.7 ± 2.0	204.7 ± 2.0	84.0 ± 0.6
HIP 68933	24/5/15	S	-16.9 ± 4.3	39.1 ± 4.3	42.6 ± 4.3	56.7 ± 5.8
HIP 71352	12/5/14	S	5987.4 ± 3.6	-1757.4 ± 3.1	6240.0 ± 3.4	171.8 ± 0.0
HIP 71683	12/5/14	S	30.3 ± 3.2	-30.0 ± 2.1	42.6 ± 2.7	157.6 ± 3.7
HIP 72622	12/5/14	S	7.1 ± 4.2	-26.6 ± 3.6	27.5 ± 3.9	142.5 ± 8.6
HIP 74785	12/5/14	S	4.9 ± 4.1	150.5 ± 3.4	150.6 ± 3.7	44.1 ± 1.6
HIP 74946	12/5/14	S	3.3 ± 4.8	-29.4 ± 4.1	29.5 ± 4.4	138.2 ± 9.2
HIP 77952	9/2/14, 22/5/15	S	5.3 ± 4.4	3.7 ± 4.2	6.4 ± 4.3	17.5 ± 37.9
HIP 79593	12/5/14, 24/5/15	S	-50.1 ± 4.7	-480.1 ± 4.2	482.7 ± 4.5	132.0 ± 0.6
HIP 82396	1/9/14	S	10.5 ± 6.6	27.0 ± 9.2	28.9 ± 7.9	34.4 ± 13.8
HIP 84012	12/5/14	S	25.2 ± 4.4	-50.7 ± 3.8	56.6 ± 4.1	148.2 ± 4.4
HIP 85792	12/5/14	S	5113.8 ± 4.0	-1469.1 ± 3.5	5320.6 ± 3.8	172.0 ± 0.0
HIP 86228	12/5/14	S	-149.3 ± 3.6	-21.3 ± 3.0	150.8 ± 3.3	94.1 ± 1.2
HIP 88635	1/9/14	S	37.6 ± 20.3	-8.3 ± 14.7	38.5 ± 17.5	173.8 ± 22.4
HIP 89931	12/5/14	S	-313.1 ± 5.1	-502.5 ± 4.5	592.1 ± 4.8	119.0 ± 0.5
HIP 90185	1/9/14	S	38.8 ± 4.5	158.2 ± 4.3	162.9 ± 4.4	38.1 ± 1.6
HIP 90496	1/9/14	S	9.6 ± 10.0	-53.4 ± 9.1	54.2 ± 9.5	140.1 ± 10.5
HIP 92855	1/9/14, 22/5/15	S	-30.7 ± 3.5	-166.9 ± 3.4	169.7 ± 3.4	129.8 ± 1.2
HIP 93506	1/9/14	S	0.9 ± 4.6	-28.2 ± 4.7	28.2 ± 4.6	135.9 ± 9.3
HIP 100751	1/9/14	S	-5.7 ± 4.8	-85.5 ± 4.1	85.6 ± 4.4	133.1 ± 3.2
HIP 107556	1/9/14	S	2.4 ± 19.8	-29.5 ± 15.6	29.6 ± 17.7	137.3 ± 38.3
HIP 109268	31/8/14	D	-91.4 ± 3.4	21.1 ± 3.1	93.8 ± 3.3	83.5 ± 1.9
HIP 110130	31/8/14, 26/6/15	D, S	-107.4 ± 1.8	-74.7 ± 4.2	131.1 ± 4.2	107.4 ± 1.8
HIP 112122	1/9/14	S	330.7 ± 5.8	560.2 ± 8.1	650.5 ± 7.0	29.7 ± 0.6
HIP 113368	28/8/14	D	-17.8 ± 3.2	-16.6 ± 3.0	24.3 ± 3.1	111.5 ± 7.4

Notes. ^aHyphenation indicates object was observed once per day inclusive.

^bCalibration type: full sky subtraction (S), or dark subtraction only (D).

^cSirius was used as a low polarization standard.

(Section 4.8) before concluding with a look at the remainder of B stars (Section 4.9). Finally, we consider the late giants in the survey (Section 4.10).

4.1 Comparison with previous observations

Of the stars highlighted in Section 2.1 as having previous significant polarization measurements, all have significant measurements

in our survey also. Our determinations are all of the same order of magnitude as the previous ones. However, all are significantly different. This is reflective either of the improved precision of HIPPI over older instruments, or these three stars are variable in polarization – an indication that the polarization is intrinsic. A less likely possibility is that the variation represents the movement of the stars with respect to the patchy interstellar medium, but the variability we see would correspond to the movement of many tens of parsecs

worth of dust based on the polarization with distance relation found by Bailey et al. (2010) for Northern stars.

The best match for previous measurements is with that of Tinbergen (1982) for Spica, where we are in agreement within the error for both previous measurements in q and significantly different to less than 2σ in u . The measurement tabulated by Heiles (2000) is half the degree of polarization and 63° different. Spica will be discussed in detail in Section 4.7.1.

For the late Giant δ Sgr, we are in agreement with Tinbergen (1982) in u , but have a thrice greater q measurement that is significant to more than 3σ . For β Gru, we have double the polarization of Heiles (2000) and a polarization angle that is 126° different, again this is significant to more than 3σ . This is strong evidence for variable intrinsic polarization. These two stars will be discussed in Section 4.10.

4.1.1 Sirius

Like Bailey et al. (2015), we have used Sirius as a low polarization standard, and in fact combined the measurements reported there with additional observations. We now make its polarization as 5.5 ± 1.7 ppm. From the discussion below in Section 4.3, it will be seen that this is entirely consistent with interstellar polarization at Southern declinations. At 2.6 pc distant and a V magnitude of -1.46 , Sirius is a particularly good unpolarized standard for instruments that can tolerate its brilliance. It should be pointed out though that the white dwarf companion, Sirius B, is currently separated from the primary by $10:2$ arcsec (Burnham 1978a) and well outside the $6:7$ arcsec HIPPI aperture. Care will need to be taken with larger instrument apertures or closer to periastron (which next occurs in 2044) when the separation is 3 arcsec (Burnham 1978a).

4.2 Survey statistics

In Table 6, the polarization properties as a function of spectral type for both this work and the survey conducted by Bailey et al. (2010) with PlanetPol are listed for comparison. The PlanetPol instrument operated with a very broad-band red filter covering the wavelength range from 590 nm to the detector cutoff at about 1000 nm (Hough et al. 2006) – redder than our measurements made with HIPPI. The empirical wavelength dependence of interstellar polarization is given by *Serkowski's Law* (Wilking, Lebofsky & Rieke 1982):

$$p(\lambda/\lambda_{\max}) = \exp((0.1 - 1.86\lambda_{\max}) \ln^2(\lambda/\lambda_{\max})), \quad (1)$$

where λ is the wavelength examined and λ_{\max} the wavelength of maximum polarization. A typical value for λ_{\max} is 550 nm (Serkowski, Mathewson & Ford 1975), and for the effective wavelength of a G0 star observed by HIPPI and PlanetPol this

Table 6. Polarization for spectral classes.

Spectral class	HIPPI ^a			PlanetPol ^b		
	N	Mean d (pc)	Median p (ppm)	N	Mean d (pc)	Median p (ppm)
B ^c	9	65.0	145.7	5	49.6	36.8
A	14	31.7	29.6	18	28.1	8.4
F/G	10	45.5	32.9	9	23.5	9.4
K	9	40.9	54.2	12	38.7	9.8
M	4	49.1	263.6	4	78.6	109.2

Notes. ^aThis work.

^bBailey et al. (2010).

^cBe stars not included for HIPPI; if included: 13, 67.3, 166.6.

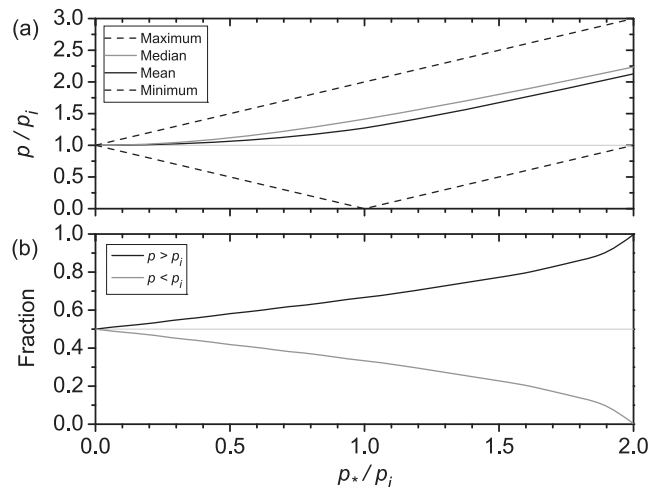


Figure 1. (a) How the polarization measured, p , changes as the ratio of intrinsic to interstellar components, p_*/p_i . The range of values between the plotted maximum and minimum (dashed) are possible, but for a sufficiently large sample the mean (black) and median (grey) p will always be greater than p_i for a non-zero p_* . (b) As p_*/p_i increases the probability of a random measurement of p for a star being greater than p_i increases.

corresponds to a factor 1.08 times greater polarization for HIPPI. However, extremes in λ_{\max} can range from 340 to 1000 nm. The difficulty in measuring polarization to the ppm level has so far prevented λ_{\max} from being determined within 100 pc.

Before analysing Table 6, it is pertinent to briefly discuss the statistics of the degree of polarization in such a survey as this. The degree of polarization of a system, p , is the vector sum of intrinsic, p_* , and interstellar, p_i , components; from the Law of Cosines:

$$p = \sqrt{p_i^2 + p_*^2 - 2p_i p_* \cos(\pi - 2\alpha)}, \quad (2)$$

where α is the angle of interstellar polarization relative to the direction of the intrinsic component. As we do not know the orientation of either component of polarization, α will have a random value between 0 and π . Fig. 1(a) shows how this effects polarization measured as a function of the ratio of intrinsic to interstellar polarization. If the intrinsic component of polarization is more than twice the interstellar component, then the polarization measured will always be greater than p_i . However, even for relatively small values of p_* , on the average we expect p to be greater than p_i , even if a fraction of polarizations measured are less than the degree of interstellar polarization – as shown in Fig. 1(b).

From Table 6, the median polarization is similar across the spectral classes A, F, G and K for both instruments. Tinbergen (1982) suspected the presence of variable intrinsic polarization at the 10^{-4} level in stars with spectral type F0 and later. This supposition was not supported by the more sensitive observations of Bailey et al. (2010). Higher polarizations were indicated for spectral classes B and M, but they had very few stars of those types, and at larger average distances, and so could not ascribe that to any intrinsic polarization of those stars.

Adding our results to those obtained with PlanetPol makes it clear that B and M spectral classes do have higher polarizations; this is true even if we discount the Be stars. As is to be expected from our selected V magnitude limit of 3.0 the B stars are on average at larger distances than those of other spectral classes – more than twice the mean distance than for A stars – yet the median polarization is more than four times that of the A stars. We have fewer M stars,

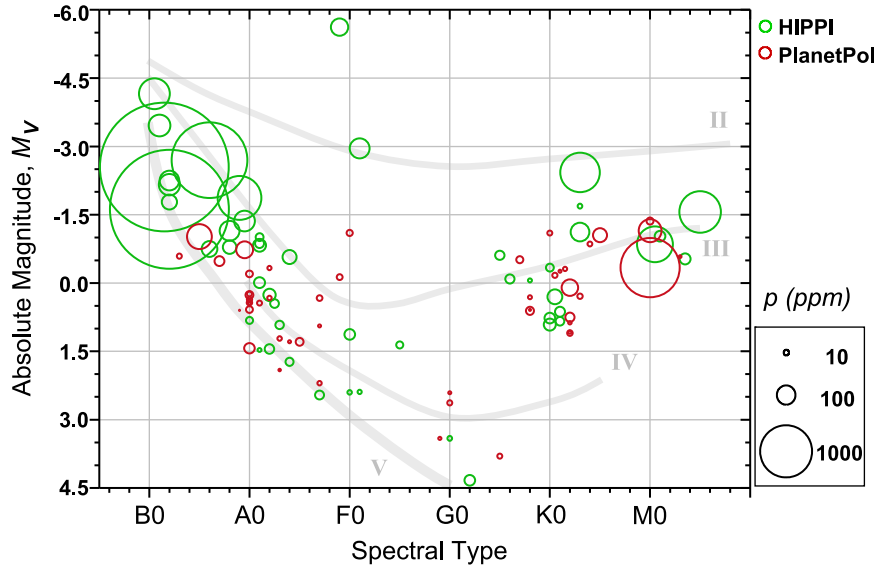


Figure 2. The results of both the HIPPI (green) and PlanetPol (red) surveys plotted on a H-R Diagram. The degree of polarization detected is represented by the area of the bubble. The main sequence (V), subgiant (IV), giant (III) and bright giant (II) branches are indicated. Two clear trends are observed: (1) increased polarization of B stars, and (2) increased polarization of late giant stars.

together with the PlanetPol only eight, but three of them have a polarization of ~ 500 ppm or greater. Additionally, the furthest K giant (K3III), δ Sgr, also has a polarization in excess of 500 ppm. As will be discussed later, the interstellar contribution is not likely to be much more than 150 ppm even at 100 pc, and so a measurement of 500 ppm, in addition to the variability observed with respect to the observations of Tinbergen (1982), strongly argues for an intrinsic cause.

Plotting the polarization for all stars observed by us and Bailey et al. (2010) on a H-R Diagram (Fig. 2) best illustrates the trends with spectral type. Even if one ignores the highest polarizations of the four Be stars, it can be seen that there is a stark contrast around spectral type A0, where earlier types have a greater degree of polarization. The sharpness of the division between A and B stars suggests an intrinsic mechanism or mechanisms particular to this stellar type; this will be discussed in Section 4.9.

On the giant branch (luminosity class III), we have very sparse data earlier than G5. For later types, and greater luminosities, there is a trend towards higher polarizations. In Section 4.10, we identify a number of K and M giants that we can be reasonably certain are intrinsically polarized and investigate the most likely mechanisms.

4.3 Polarization spatial distribution

To investigate the spatial distribution of interstellar polarization, we have plotted PlanetPol and HIPPI survey stars' polarization degree and angle in equatorial co-ordinates (Fig. 3) and projected on to Galactic co-ordinates (Fig. 4). B type stars, M type stars and the K giant σ Sgr have been neglected to reduce contamination from intrinsic polarization.

The PlanetPol survey (Bailey et al. 2010) found low interstellar polarization towards the Galactic north pole, with higher polarizations below 40° Galactic latitude towards the Galactic Centre⁵, and

that in this range there was a tendency for alignment in the Galactic plane. Removing the B and M stars has not changed that picture (Fig. 4). The new results we present here align well with those of PlanetPol. The few data points we add at high Galactic latitudes are relatively low polarization. Near the Galactic Centre, we add data at lower Northern Galactic latitudes; the polarization vectors for these data points between $l = \sim 0^\circ$ and 120° show an alignment consistent with the PlanetPol data, i.e. along the Galactic plane. Further south a different picture emerges.

Our survey has added significantly more data points in the Galactic south. Even if one allows for the wavelength difference between HIPPI using the g' filter and PlanetPol's 600–800 nm window, in general Southern stars appear significantly more polarized than Northern ones. That the degree of polarization is greater in the Galactic south than north is consistent with the distribution of interstellar dust clouds seen around O, B, F and G stars by *IRAS* at $60 \mu\text{m}$ (Dring et al. 1996). This might be explained by reference to the Sun's vertical displacement from the Galactic plane, z_\odot . Many studies have shown that the Sun is slightly to the north of the Galactic plane compared to its assumed position in the Galactic co-ordinate system (Joshi 2007). Thus, by observing to the south, we are looking through more of the Galactic plane where we might expect interstellar grains to be more strongly aligned and impart greater polarization.

By plotting the polarization degree per distance in Fig. 5 and with distance in Fig. 6, we can refine the picture further. We denote the polarization with distance as p/d , it is useful for comparing the degree of polarization of objects that might be separated by tens of pc. In Figs 5 and 6, the polarization has been debiased as $\sqrt{p^2 - \sigma^2}$. Bailey et al. (2010) noted at right ascensions greater than 17 h a p/d relation of $\sim 2 \times 10^{-6} \text{ pc}^{-1}$. With the removal of the B and M stars from the map, there remain only three stars supporting this trend for declinations greater than 30° . One of these is Vega, which we can discount from considerations of interstellar polarization on the basis

⁵ It should be pointed out that the spatial scale of measurements made by PlanetPol and HIPPI is many orders of magnitude less than the Galactic scale, and that in this case a maximum seen towards the Galactic Centre is

coincidental. The Solar System is currently located between the Orion Spur and the Sagittarius Main Arm.

of its large debris disc. The remaining two stars are the K giants γ Dra and κ Lyr. From the discussion that follows in Section 4.10, it is likely that these stars are also intrinsically polarized. Indeed, cross-reference between Figs 3 and 5 reveals the position angles of these three stars do not match those nearby. Given that they all lie near the Galactic equator, where there is otherwise a good measure of alignment, the case is strong for intrinsic polarization.

The large degree of polarization observed for α Cen is probably not real, and is discussed in detail in Section 3.1. From our survey, two further K giants, α Phe and α Tuc, can be identified as probably intrinsically polarized, as they have a p/d greater than any other stars within 100 pc. What remains is a region of low p/d centred on 14 h right ascension, $+35^\circ$ declination – this region was mostly covered by the PlanetPol survey – indicating a relatively dust free volume. Within this region stars are polarized at $\sim 2 \times 10^{-7}$ pc $^{-1}$. Further South and East p/d is greater, and somewhat patchy. The stars with the greatest p/d tend to lie within -15° and -30° declination or nearby; these stars are polarized at $\sim 2 \times 10^{-6}$ pc $^{-1}$. Between the two regions are stars with intermediate polarizations. A linear fit to stars from our survey not suspected of being intrinsically polarized gives 1.14×10^{-6} pc $^{-1}$ with a coefficient of determination, $R^2 = 0.67$. The highly polarized Southern stars for the most part lie within 30 pc. Though we have fewer stars further away, these are mostly less polarized. This suggests that the higher interstellar polarization of Southern stars is imparted predominantly by nearby dust lying, from Fig. 6, between 10 and 30 pc distant. Coincidentally, the majority of estimates for z_\odot place the Sun 15 to 30 pc above the Galactic plane (Joshi 2007), though the implication is most likely a local dust cloud at this distance.

The polarization of more distant stars in the interstellar medium has been shown to increase with distance as $\sim 2 \times 10^{-5}$ pc $^{-1}$ (Behr 1959). That nearby stars show less polarization was demonstrated by Tinbergen (1982) and Leroy (1993b). Exactly how much less was determined by Bailey et al. (2010) for Northern stars in the PlanetPol survey. Bailey et al. (2010) believed that the furthest stars in their survey showed high polarizations as a result of their proximity to the wall of the Local Bubble. As a result of the work presented here, we now believe those stars to be polarized by intrinsic processes. The two furthest stars shown in the figures are Canopus and θ Sco from our survey; they exhibit the greatest degree of polarization. This may be due to these stars being beyond the wall of the Local Bubble. Repeat observations of Canopus do not show any variation (Bailey et al. 2015), which supports this. However, they are also the most luminous non-B stars in the survey, and to the best of our knowledge the polarization of close bright giants at the ppm level has not previously been investigated (though it should be noted that early-type supergiants do display intrinsic aperiodic variable polarization arising as a result of asymmetric mass-loss Hayes 1984, 1986). The third magnitude limit in V for this survey has resulted in fewer main sequence and subgiant stars at distance than the PlanetPol survey with its limit of fifth magnitude. Without more data it is not possible to say definitively whether we are probing the wall of the Local Bubble with our furthest stars.

4.4 Debris discs

Debris discs are circumstellar discs of dust around main-sequence stars. They are typically detected and characterized by excess infrared emission above that of the stellar photospheric continuum emission. The peak wavelength of dust emission from debris discs depends primarily on the distance from the star (Matthews et al. 2014). Broadly speaking, two typical temperature regimes are ob-

served; warm dust (T_d 150–220 K) analogous to the Asteroid belt, and cold dust ($T_d \sim 50$ –80 K) analogous to the Edgeworth–Kuiper belt (Morales et al. 2011). Edgeworth–Kuiper belt analogues are more easily detected by this method than closer discs owing to the greater contribution of the stellar photosphere to the total emission at mid-infrared wavelengths. Recent far-infrared surveys with the PACS instrument (Poglitsch et al. 2010) on the *Herschel Space Observatory* (Pilbratt et al. 2010), where detection is already sensitivity limited, have found debris discs for up to 33 per cent of A stars (Thureau et al. 2014), and 20 per cent of FGK stars (Eiroa et al. 2013). The ratio of the luminosity of the disc to that of the star, F_{IR}/F_* , is indicative of the total starlight intercepted by the debris disc (Wyatt 2008), but by itself is not a reliable predictor of scattered light brightness (Schneider et al. 2014). The spectral energy distribution of a debris disc is also a function of the dust particle size distribution and composition as well as its architecture. Dust particles in circumstellar discs polarize light by scattering and absorption processes, and sensitive polarimetry is potentially useful for removing degeneracies (Schneider et al. 2014; García & Gómez 2015). Polarization seen by aperture polarimetry – where the aperture takes in the central star as well as the whole/a large portion of the disc – has been reported at levels of ~ 0.1 –2 per cent (García & Gómez 2015 and references therein).

As part of our survey, we observed four main-sequence objects thought to be debris disc host stars, namely: Fomalhaut (HIP 113368), ι Cen (HIP 65109), β TrA (HIP 77952) and γ TrA (HIP 74946). The PlanetPol survey also observed five debris disc systems: Vega (BS 7001), Merak (BS 4295), γ Oph (BS 6629), β Leo (BS 4534) and α CrB (BS 5793). Concurrently with the bright star survey, we carried out another programme where we observed debris disc systems. What can be learned from all of these observations has been substantially dealt within another paper (Marshall et al. in preparation). In brief, comparison of the polarization with measurements of the discs’ thermal emission demonstrate the capacity for polarization measurements to constrain the geometry and orientation of unresolved debris discs. A typical ratio of polarization to thermal emission of between 5 and 50 per cent, consistent with scattered light imaging measurements. The majority of discs in the sample have polarization signals aligned approximately perpendicular to the disc major axis, indicative of scattering from the limb of small grains in those discs. No trend was found in the polarization with either disc inclination, nor luminosity of the host star. The characterization of the system β TrA as debris disc system based on a far-infrared excess derived from a single waveband *IRAS* measurement is found to be unreliable.

What remains to be presented here is a comparison of polarization in these debris disc systems compared with those of the other main-sequence stars in the survey, this is shown in Table 7. If the contribution from the disc is greater than the interstellar polarization then it is obvious that we would expect a higher polarization on average from debris disc systems. Yet geometrical considerations related to the vector sum of intrinsic and interstellar components mean we should also expect a slightly higher polarization from debris disc systems on average when the magnitude of contributions is similar or even smaller (as detailed in Fig. 1). The situation is depicted graphically in Fig. 7.

The analysis of the PlanetPol survey data is presented here for the first time. In the PlanetPol data, debris disc systems show slightly higher median polarizations at shorter average distances. If one were to apply the p/d relation established by Bailey et al. (2010) for stars between 10 and 17 h RA in the PlanetPol survey, then one would expect 3.8 ppm at 19.0 pc. However as both the debris disc

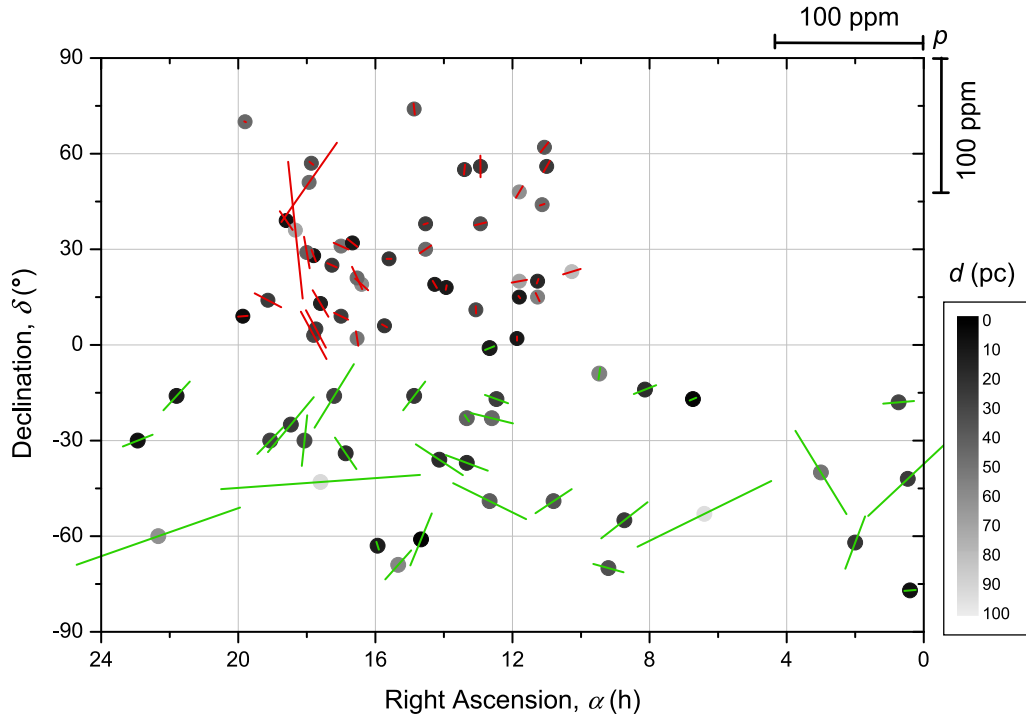


Figure 3. A–K stars within 100 pc from the HIPPI (green) and PlanetPol (red) surveys plotted on an equatorial co-ordinate system. Stellar positions are marked by dots, with a grey-scale indicating distance from the Sun in pc. Vectors denote the degree and angle of the polarization.

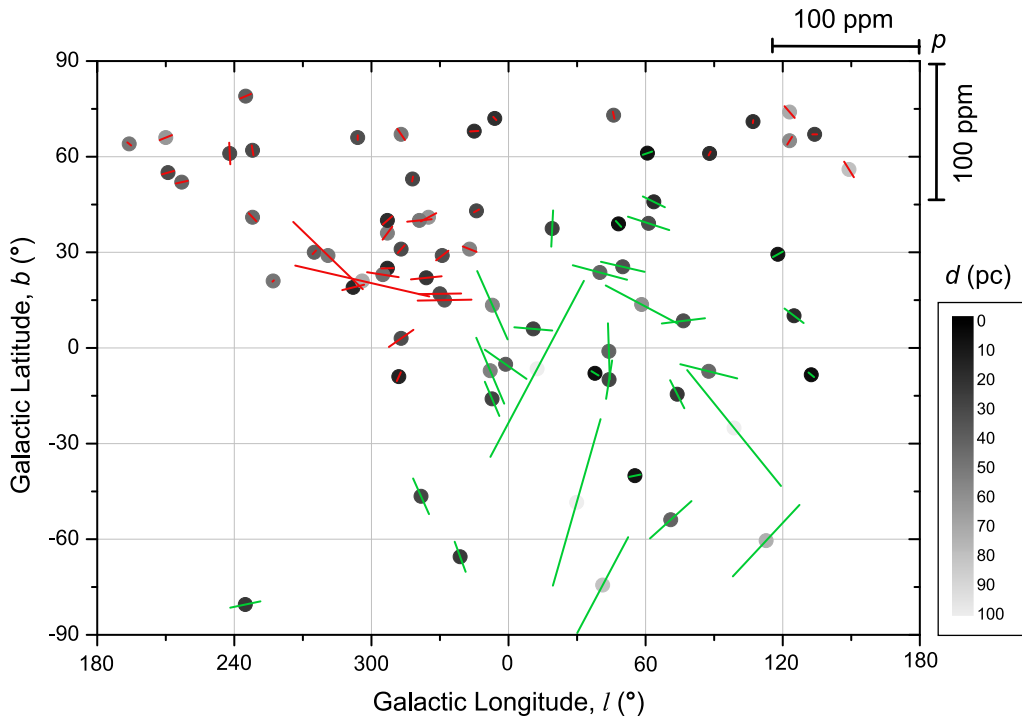


Figure 4. A–K stars within 100 pc from the HIPPI (green) and PlanetPol (red) surveys plotted on Galactic co-ordinates. Stellar positions are marked by dots, with a grey-scale indicating distance from the Sun in pc. Vectors denote the degree and angle of the polarization.

and main-sequence samples contain stars with greater RA, a more cautious value of 5.1 ppm is achieved by scaling the p/d from the other class V stars. The relation described by Fig. 7 then gives us a median polarization contribution from debris discs in the PlanetPol sample of 8.1 ppm. Given PlanetPol’s 5 arcsec aperture would not

often capture the full disc for such close objects this is in line with expectations.

In the HIPPI data, we have a higher polarization for debris discs, but at a larger average distance. However γ TrA has a tiny infrared excess and would not be expected to have much of a polarization

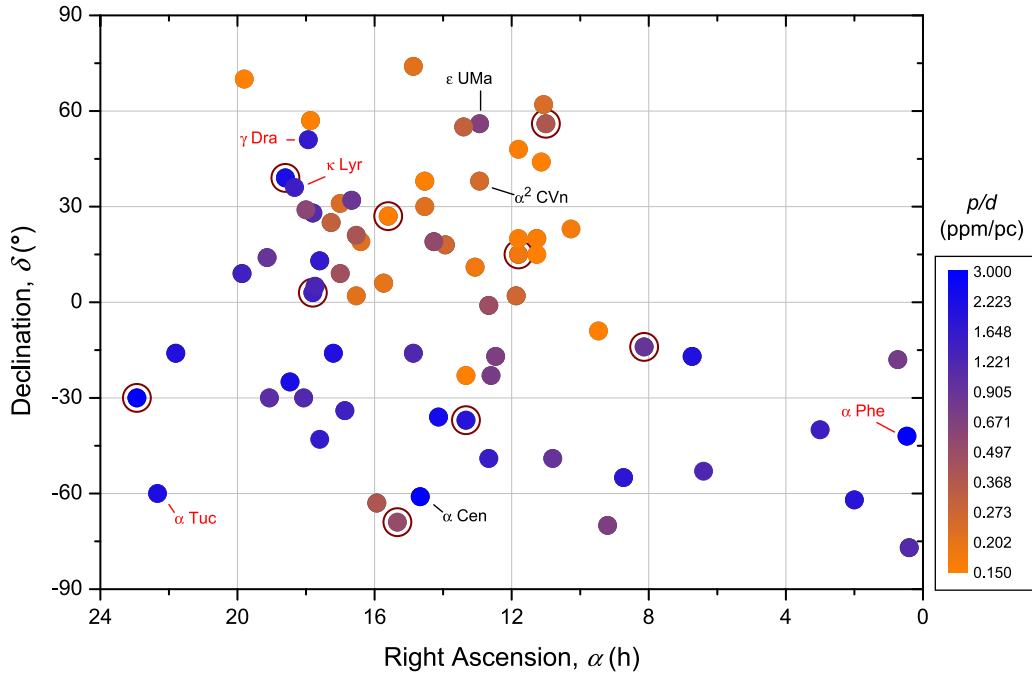


Figure 5. A–K stars within 100 pc from the HIPPI and PlanetPol surveys plotted on an equatorial co-ordinate system. Stellar positions are marked by dots. Polarization with distance, p/d , in ppm/pc is given by the colour scale to align with Fig. 6. Brown rings denote debris disc stars. Stars labelled in red are K giants that may be intrinsically polarized. Stars labelled in black may not be representative of interstellar polarization for other reasons (see the text).

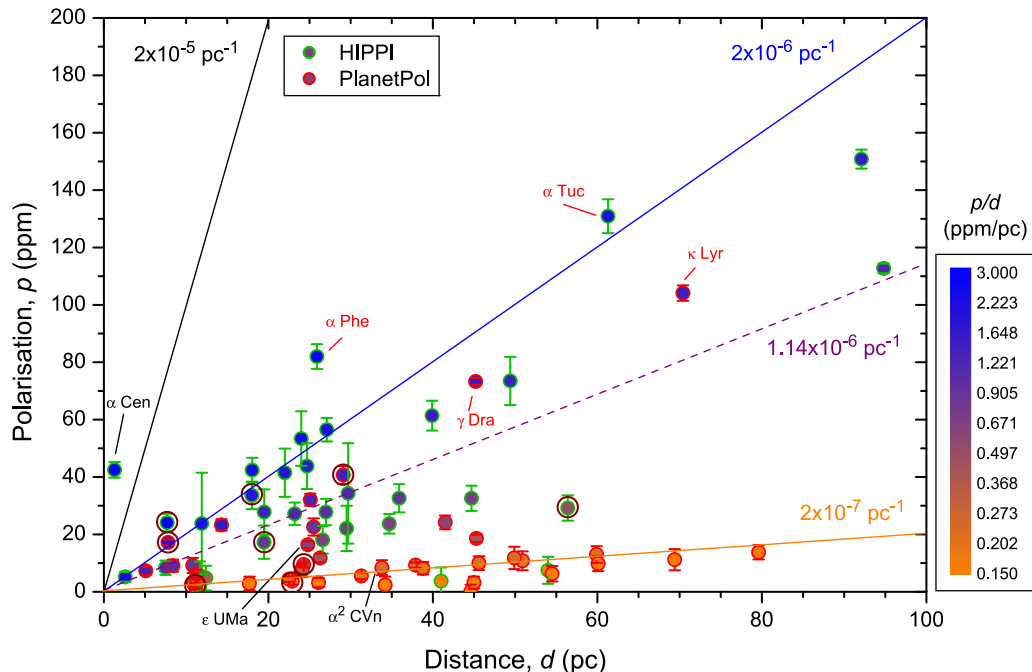


Figure 6. Polarization with distance, p/d , for A–K stars within 100 pc from the HIPPI (green) and PlanetPol (red) surveys. Stellar positions are marked by dots. Polarization with distance in ppm/pc is given by the colour scale to align with Fig. 5. Brown rings denote debris disc stars. Stars labelled in red are K giants that may be intrinsically polarized. Stars labelled in black may not be representative of interstellar polarization for other reasons (see the text). The dashed line represents a linear fit to the unannotated HIPPI stars.

signal, maybe 5 ppm at most (Marshall et al. in preparation), and yet at 56 pc it is contributing most to the mean distance. The other two disc systems together have a median polarization of 29.1 ppm at a mean distance of 12.9 pc, which given their median excess of $F_{\text{IR}}/F_{\star} = 18 \times 10^{-6}$ (Marshall et al. in preparation) is more

in line with expectations. However, the very small numbers of debris disc systems (and also other main-sequence stars) means that it is difficult to draw conclusions at this level, particularly in light of an uncertain contribution from the local interstellar medium (Section 4.3).

Table 7. Polarization for debris disc and non-debris disc main-sequence stars.

Type	HIPPI ^a			PlanetPol ^b		
	<i>N</i>	Mean <i>d</i> (pc)	Median <i>p</i> (ppm)	<i>N</i>	Mean <i>d</i> (pc)	Median <i>p</i> (ppm)
Debris disc ^c	3	27.4	29.5	5	19.0	9.6
Other class ∇^d	6	16.2	18.1	11	33.0	8.8

Notes. ^aThis work.

^bBailey et al. (2010).

^cIf γ TrA in HIPPI survey is excluded: 2, 12.9, 29.1.

^dA–K stars only. Does not include α Cen in HIPPI survey (see Section 3.1.1); if included: 7, 14.1, 27.5.

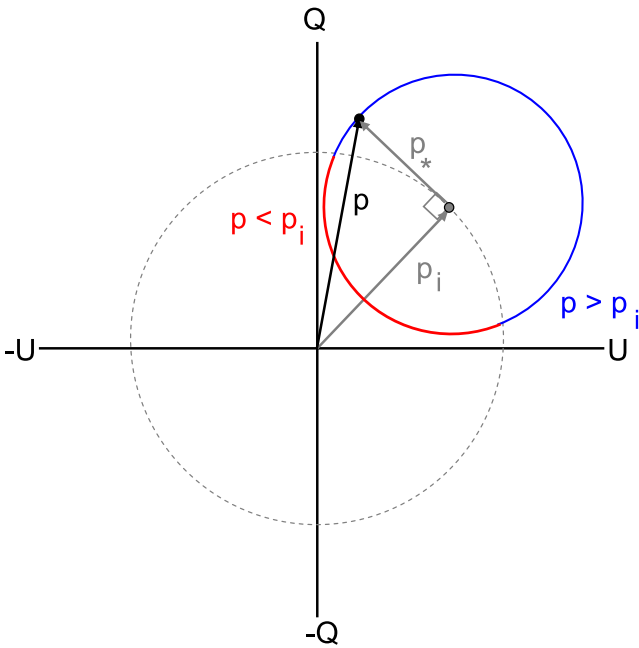


Figure 7. The vector sum, p , of interstellar, p_i , and intrinsic, p_* , components of polarization shown in the $Q - U$ plane. The situation where the sum is less than the interstellar polarization by itself is represented by the red arc; the situation where it is greater is represented by the blue arc. Given a random distribution, more points will lie on the blue arc than the red and thus the average p will be greater than p_i . The polarization is equivalent to the median when p_* is perpendicular to p_i , and then equation (2) reduces to $p_* = \sqrt{p^2 - p_i^2}$.

Comparison of Figs 3 and 5 reveals four of the eight debris disc systems to have polarization angles closely aligned with their nearest neighbour stars in the survey. This naturally leads to two hypotheses: (1) that interstellar polarization is swamping the contribution from the disc, or that (2) the local interstellar magnetic field plays a role in the formation of the system. In this instance both of these may be discounted by consideration of the individual systems. The four systems with similar alignment are Fomalhaut, ι Cen, Merak and γ Oph. Taking the second hypothesis first, this would seem most probable if the systems were young and had formed near to where they are now. None of them is particularly young though. Furthermore, the HIPPI aperture does not encompass the whole disc of Fomalhaut nor Merak. Meaning that the position angle we have measured does not correspond to the minor axis of the disc for either of these systems (Marshall et al. in preparation).

The contribution of the interstellar polarization to that measured for the debris disc systems is harder to gauge without more precise data from nearby systems. Certainly, the data presented in Table 7 suggest that the interstellar contribution could be significant. A number of factors argue against interstellar polarization being dominant though. In the case of Fomalhaut, the p/d is 3.06 ppm pc^{-1} , higher than for any other survey star identified as having interstellar polarization alone. For ι Cen, we have obtained data in different wavelength bands as part of another project (Marshall et al., unpublished data); preliminary analysis of these data gives a wavelength dependence inconsistent with interstellar polarization (Serkowski 1973; Oudmaijer et al. 2001). For γ Oph, the polarization angle measured is very well aligned with the minor axis of the disc determined from imaging (Marshall et al. in preparation), making the interstellar contribution very difficult to gauge. The PlanetPol measurements of Merak and β Leo are consistent with interstellar polarization – β Leo has a polarization of only $2.3 \pm 1.1 \text{ ppm}$ and we have, on occasion, used it as a low polarization standard – and it could be the characteristics of the discs in these two systems do not generate significant polarization. For a fuller discussion of factors contributing to debris disc polarization see Marshall et al. (in preparation).

4.4.1 Altair

Altair (BS 7557, α Aql), observed as part of the PlanetPol survey (Bailey et al. 2010), though not a classical debris disc system, has been identified as having an infrared excess through interferometric measurement of the star at near-infrared wavelengths (Absil et al. 2013). Based on the spectral slope of the excess, it was predicted that the excess was attributable to scattered light rather than thermal emission. Given that small dust grains should be more effective scatterers at shorter wavelengths an appreciable polarization would have been expected. The PlanetPol measurement is consistent with the contribution from the interstellar medium. From this, we might infer that the grains responsible for scattering could well be too small to be effective polarizers, i.e. nanoscale dust grains as postulated by Su et al. (2013).

4.4.2 ρ Pup

Another non-traditional disc system is the bright giant ρ Pup (HIP 39757, F5II). It was identified as having a debris disc by Rhee et al. (2007), with a $60 \mu\text{m}$ excess of $5 \pm 1 \times 10^{-6}$; it has an even more significant excess according to McDonald et al. (2012) of 160.7×10^{-6} . The degree of polarization measured, 18.3 ppm, is consistent with what is expected from its infrared excess (Marshall et al. in preparation). However, there are no imaging data available to gauge its geometry or confirm that the dust present is in the form of a traditional debris disc. The system is 18.3 pc distant, positioned on the border of the low and high polarization regions in Fig. 5, and so it is difficult to determine the relative contributions of the interstellar medium and any intrinsic component due to a disc.

4.4.3 ϵ Sgr

There is one other debris disc system in the survey not mentioned up to this point: ϵ Sgr (HIP 90185). It has a high polarization measurement of $162.9 \pm 4.4 \text{ ppm}$. It is an unusual system to be discussed in the context of debris discs on two counts: (1) the primary star is a $3.52 M_{\odot}$ B giant having spectral type B9.5III, and (2) it is a binary system with the $0.95 M_{\odot}$ companion

(Hubrig et al. 2001) separated on a similar scale to the debris disc (Rodríguez & Zuckerman 2012). The secondary orbits at 106 au, whilst the disc has been detected in *IRAS* 60 μm to have an excess of 4.5×10^{-6} by Rhee et al. (2007) and is presumed to be centred at 155 au as a result (Rodríguez & Zuckerman 2012). Even greater excess has been detected with *Spitzer* at 13 and 31 μm (Chen et al. 2014; Mittal et al. 2015), implying a closer disc. The 60 μm determination places the secondary well within the HIPPI aperture, but the disc on the edge of it. ϵ Sgr was observed on 2014 September 1 when the seeing was particularly bad (~ 4 arcsec), so we probably have a large contribution to the observed polarization due to scattering from the debris disc.

What makes this system particularly interesting is that in *V* band a simple calculation shows that the contribution of the secondary to the light reaching the disc varies from ~ 0.1 per cent of the total for the furthest part to ~ 3 per cent for the closest. There is therefore an asymmetry in reflected light over the whole disc and thus in polarization as well. If the polarization we see is a result of this asymmetry then the measured polarization angle should be related to the position angle of the binary system. The position angle of the system was measured in 1999 March to be $142^\circ.3$ (Hubrig et al. 2001). Our measured polarization angle is $38^\circ.1 \pm 1^\circ.6$. When one considers that the secondary could have rotated by as much as $\sim 11^\circ$ (assuming a face-on system, a circular orbit and the formal limit on the uncertainty of the mass of component A), and that there must be contributions from interstellar polarization, it is probable that we have measured a polarization angle perpendicular to the position angle of the binary system. This is consistent with the stated hypothesis. If the system is inclined then the position angle of the binary system will not have swept through as great an angle, but we do not know precisely the interstellar contribution nor the contribution resulting from any asymmetry associated with disc inclination, so the small difference between the position angle and the expected polarization angle is not significant. More significant is that the measured infrared excess is only 11.0×10^{-6} (Mittal et al. 2015), and this should not be enough to generate this degree of polarization. However, the distance of the debris disc has been determined from the *IRAS* measurement at 60 μm and the shorter wavelength measurements made with *Spitzer* imply either a closer disc which would produce a greater asymmetry, or a circumsecondary disc as has been suggested for the HD 142527 system (Rodigas et al. 2014).

Based on the *IRAS* and *Spitzer* data, we modelled the spectral energy distribution of the system using two blackbody components and obtained an fractional excess of 31×10^{-6} , which is more consistent with what we would expect based on the polarization measured. The quality of this value is strongly dependent on the assumptions made regarding the temperature of the cold component and the stellar photosphere contribution. The stellar photosphere was represented by a Castelli–Kurucz model (Castelli & Kurucz 2004) with an effective temperature of 10 000 K and a surface gravity, $\log g$, of 4, and solar metallicity. This was scaled to the optical and near-infrared photometry from SIMBAD. In our model, we fixed the temperature of the cold component to 85 K, such that its emission peaked at 60 μm – the wavelength of the longest reported flux density measurement. The warm component was fitted to the mid-infrared excess, which resulted in a temperature of 300 K. The combined model overestimates the flux density at 31 μm compared to that reported by Chen et al. (2014). Due to the absence of longer wavelength data constraining the peak of the cold emission, the total fractional excess is subject to large uncertainties.

At this point, it should be noted that ϵ Sgr B was found as a result of a search of late-B stars showing high X-ray fluxes (Hubrig

et al. 2001). Some X-ray binaries have been found to show variable polarization (Clarke 2010) and so this is an alternative explanation for the polarization observed. However, such detections have been rare, and generally for much stronger X-ray sources. Considering the magnitude of the flux asymmetry induced by the secondary, scattering from the debris disc seems the most likely mechanism. Indeed the X-ray activity might be an indication of dust accretion on to the secondary, which is another scenario suggested for HD 142527 (Rodigas et al. 2014).

Presuming the polarization we see in this system is a result of scattering from the disc, then the behaviour with wavelength will be a function of the ratio from components A and B, as well as the properties of the grains in the disc. The polarization will likely be greater at redder wavelengths than typical for a debris disc system. If the secondary is interior to the disc, as it orbits it will race ahead of the disc, illuminating each section in succession as if a torch shinning upon it. Follow up observations of this object offer a unique opportunity to use polarization to probe the radial homogeneity of the debris disc. Though it will take some time.

4.5 Ap stars

As an aside, from Fig. 5 it is clear that ϵ UMa (BS 4905) is more polarized than the stars around it. ϵ UMa has spectral type A1III–IVp and is the brightest chemically peculiar star in the sky. Ap stars typically exhibit high degrees of polarization as a result of magnetic fields in the many hundreds of Gauss (Clarke 2010). Such fields generating broad-band polarization through, for example, differential saturation of Zeeman components as described by Leroy (1990). ϵ UMa has a strong magnetic field, and a rotational axis at an angle to its magnetic axis that periodically brings its magnetic pole into line of sight; this is the likely cause of its high degree of polarization. However, recently it was proposed that the periodicity displayed (5.0887 d) by the star is a consequence of a 14.7 M_J companion orbiting at a distance of 0.055 au (Sokolov 2008), and this could also be a contributor.

There is one other Ap star in the PlanetPol survey: α^2 CVn. This star is known to have a regular time varying polarization. Recent broad-band measurements in a similar range to that of PlanetPol have shown that the degree of linear polarization varies between zero and more than 0.7 per cent (Kochukhov & Wade 2010). It thus appears a matter of chance that the recorded degree of polarization for α^2 CVn by PlanetPol was just 8.8 ppm.

4.6 Eclipsing binaries

The work credited with bringing about the beginning of stellar polarimetry in earnest is that of Chandrasekhar (1946)⁶. In this work, he described how polarization arising from free electron scattering at the limb of a star might be observed by using an eclipsing binary to break the symmetry of the stellar disc. It was shown that the limb would be most polarized with the azimuth of vibrations tangential to the limb, and that the polarization would fall away quickly from there, becoming zero in the centre of the stellar disc. Usually the symmetry of the stellar disc renders this effect undetectable in aperture polarimetry, but an eclipsing binary breaks the symmetry. The magnitude of the limb polarization varies depending on the type of star, with earlier types showing greater polarization (Kostogryz & Berdyugina 2015). Measurements of polarization across the disc of

⁶ The serendipitous discovery of interstellar polarization was made in the process of searching for the *Chandrasekhar Effect* (Clarke 2010).

the Sun were first used to confirm the effect, and the Sun has a maximum limb polarization of ~ 12 per cent (Kostogryz & Berdyugina 2015).

There is one eclipsing binary in our survey, δ Cap (HIP 107556, A7III). This star also happens to be chemically peculiar. The G type secondary has an orbital period of 1.022 789 d (Eggleton & Tokovinin 2008). It is noteworthy that the error associated with our measurement of δ Cap is larger than any other in the survey. This could be the result of observing the system during a transit or transitioning into or out of secondary eclipse producing variable limb polarization effects. However, the weather was variable on the night of the observation, and it is equally likely that the large error is associated with reduced signal from patchy cloud.

The star α CrB (BS 5793, A0V) observed in the PlanetPol survey is also an eclipsing binary of the Algol type (Eggleton & Tokovinin 2008), but does not show any polarimetric behaviour from those observations of note.

4.7 Close binaries

Variable polarization can occur in close binary systems as a result of light scattered from material co-rotating in the system or from emission line effects associated with stellar winds or gaseous streams (Clarke 2010). A common property of many early-type close binary systems is the presence of a gaseous extrastellar envelope, possibly of protosolar material (McLean 1980). The dynamics of a binary system render this envelope asymmetric, resulting in an intrinsic polarization signal that varies with the binary phase according to the system geometry with respect to the observer and the polarigenic mechanism (McLean 1980). The requirement for extrastellar material resulted in a divide between evolved and unevolved stars when investigated by Pfeiffer & Koch (1977). Having investigated systems with separations up to ~ 5 au, they found binaries with unevolved stars, with few exceptions, do not show intrinsic polarization; whilst those with evolved stars are likely to be intrinsically polarized if the pair are separated by more than 10 solar radii ($10 R_{\odot}$). Pfeiffer & Koch (1977) hypothesized that the $10 R_{\odot}$ divide resulted from insufficient material being present to generate a large enough signal to be detectable by the instrumentation of the time (that being $\sim 10^{-4}$).

Within our survey there are a three B-type primaries with close companions, these being HIP 60718 (α Cru – as already mentioned in Section 3.1.2), HIP 100751 (α Pav) and HIP 65474 (Spica). All three show significant polarizations.

4.7.1 Spica

Spica is classified as B1III-IV and has a B2V companion with an orbital period of just 4.014 5898 d (Harrington et al. 2009). It is Beta Cephei-type variable star that varies in brightness with a 0.1738-d period as a result of its outer layers pulsing. The brightness variability has been shown to be due to line-profile variability as a consequence of surface flows induced by tidal forces (Harrington et al. 2009).

Spica was investigated by Pfeiffer & Koch (1977) and found not to vary polarimetrically – having an observed polarization of 0.03 ± 0.01 per cent it was designated as being unpolarized. However, as our initial measurements of Spica were intermediate of those of Tinbergen (1982) given in Table 2 – even if nominally within the error in q – we considered it an interesting target to follow up. Table 8 shows the three measurements we have made of Spica. From these, it is clear that it is varying and thus intrinsically polarized.

Table 8. Individual measurements of Spica.

Date ^a	UT ^b	q (ppm)	u (ppm)	p (ppm)	θ (°)
24/5	11:02	-154.0 ± 2.5	24.7 ± 2.5	156.0 ± 2.5	85.4 ± 0.9
29/6	10:32	-185.1 ± 2.9	30.6 ± 2.8	187.6 ± 2.9	85.3 ± 0.9
29/6	12:49	-188.1 ± 3.6	57.2 ± 3.9	196.6 ± 3.8	81.6 ± 1.1

Notes. ^aAll dates are 2015.

^bThe time given as hh:mm and is that corresponding to the beginning of the measurement from the third telescope position angle in the sequence. The target was reacquired for each position angle leading to some minor variation in the timing. There was also a short pause between the middle two measurements of the third observation owing to passing cloud. Each measurement represents 24 min of data plus acquisition time.

4.8 Be stars

Be stars are defined as non-supergiants of B spectral type that have exhibited episodic Balmer line emission. The origin of the emission is attributed to the ejection of a gas circumstellar envelope (CSE) by the star (Domiciano de Souza et al. 2003). Be stars are rapid rotators that exhibit episodic mass and angular momentum losses as well as disc formation and dissipation (Domiciano de Souza et al. 2014). The rotation rate is usually said to be 70–80 per cent of the star’s critical velocity (Porter & Rivinius 2003). The stellar winds of Be stars are faster than those of ordinary B stars, particularly in earlier types. The winds are asymmetric, characterized by fast tenuous winds at the poles and stronger slower winds at equatorial latitudes.

Such stars exhibit varying polarization on both short and long time-scales. On minute to hour time-scales fluctuating polarization is attributed to ejection events, where a ‘blob’ of material is formed at the stellar surface, distorting its shape, which co-rotates with the star with the Keplerian velocity of the inner decretion disc (Carciofi et al. 2007). The extra equatorial material adds to the already distorted shape of the star caused by its subcritical rotation (which is also responsible for gravity darkening at equatorial latitudes) (Domiciano de Souza et al. 2003). On longer time-scales, a circumstellar decretion disc of ionized gas is built up around the star, the presence of which also produces an infrared excess and a non-zero (usually dominant) polarization signal according to its density and geometry – the polarization angle is aligned with the rotational axis of the star (Carciofi et al. 2007). During a quiescent phase, the disc is dissipated by radiation pressure and partial reaccretion on to the star (Carciofi et al. 2012). Be stars are known to be variable on time-scales ranging up to decades. A quiescent Be star might appear as an ordinary B star before becoming active within just a couple of days (Peters 1986; Barnsley & Steele 2013). A subclass of these objects is the B_{shell} star, where the emission lines are depressed as a result of viewing geometry, i.e. the star is equator-on to the observer (Saad, Hamdy & Abolazm 2012). However, B_{shell} behaviour is often seen intermediate of that of B and Be behaviour, suggesting the CSE may sometimes develop, at least initially, with an imperfect alignment. In such systems, polarimetry is a relatively more sensitive probe of disc development.

The definitive statistical study of Be stars and their polarization is that of Yudin (2001); Table 9 is a reproduction of the data he collated for the Be stars in our survey.

Our measurements of α Col (HIP 26634), α Ara (HIP 85792) and η Cen (HIP 71352) in the g' agree in position angle with those collated by Yudin (2001). For α Ara, Meiland et al. (2007) resolved the equatorial disc using Very Large Telescope Interferometer (VLTI)/Astronomical Multi-BEam CimbineR (AMBER) data

Table 9. Observed polarization for Be stars from Yudin (2001) compared to our measurements.

Star HIP	Yudin (2001) ^a		This work	
	p (per cent)	θ (°)	p (per cent)	θ (°)
7588	0.04	136	$0.215\ 18 \pm 0.000\ 38^b$	31.2 ± 0.1
26634	0.15 ± 0.05	109	$0.072\ 20 \pm 0.000\ 64$	101.1 ± 0.5
71352	0.61 ± 0.04	174	$0.532\ 06 \pm 0.000\ 38$	172.0 ± 0.0
85792	0.37 ± 0.07	174	$0.624\ 00 \pm 0.000\ 34$	171.8 ± 0.0

Notes. ^aNote that the tabulated values are the observed values, and that for some objects Yudin (2001) also calculated the intrinsic and interstellar components.

^bTabulated value for this work is the average of two measurements.

and calculated models with orientation in agreement with the position angle given by Yudin (2001), after subtraction of an interstellar component of 0.15 per cent at 30° to give 166° . Given the discussion in Section 4.3, this determination of the degree of interstellar polarization seems high. Meilland et al. (2012) conducted a spectropolarimetric survey of Be stars which included both α Ara and α Col. The position angle for the rotational axis of these stars was obtained by means of a axisymmetric kinematic model. The determined position angles were $88 \pm 2^\circ$ and 10° for α Ara and α Col, respectively. This places our determined position angle for the circumstellar disc of α Ara between that of Meilland et al.’s 2007 and 2012 determinations, and our measurement for α Col in closer agreement with Meilland et al. (2012) than that of Yudin (2001) is.

Our measurement for the degree of polarization of α Col is half the tabulated value indicating a smaller circumstellar disc, whereas for η Cen we record almost double the polarization level, indicating a thicker circumstellar disc. For α Ara, we record a similar level of polarization. There is no agreement for Achernar (HIP 7588) though, and as we observed it twice it bears closer scrutiny.

4.8.1 Achernar

As one of the closest brightest Be stars Achernar has been extensively studied from the 1970s onwards. During that time it has been in and out of emission – gaining and losing its disc. During the most recent period quiescent period, Domiciano de Souza et al. (2014) took advantage of a negligible disc in using interferometry to measure the position angle of Achernar’s rotational axis as 216.9 ± 0.4 . They also measured the rotational flattening of Achernar as $R_{\text{eq}}/R_p = 1.352 \pm 0.260$ making it one of the flattest fast-rotating stars. When the star is in an emission or shell state, it will have a significant disc that would be expected to lie with its major axis perpendicular to the star’s rotational axis. 36.9 ± 0.4 is thus the angle one would expect from a polarimetric measurement of the star in a disc bearing phase before any other considerations. Historic measurements of the polarization of Achernar together with our new measurements are given in Table 10.

McDavid (2005) interpreted the results of Schröder (1976) as being consistent with measuring the rotationally oblate photosphere of Achernar during a phase where the circumstellar disc was completely absent. However, the degree of polarization recorded, even allowing for uncertainty, is more than double what one would expect from the calculations of Sonneborn (1982) given Achernar’s established inclination angle of $\sim 60^\circ$ (Domiciano de Souza et al. 2014) to $\sim 65^\circ$ (Carciofi et al. 2007). Alternative explanations are that this is the interstellar component of the observed polarization, or that in the absence of the CSE it might be due to Achernar’s polar wind (Stee & Meilland 2009) or a combination of one or more of these.

Excepting that of Schröder (1976) the data in Table 10 fall into two distinct categories: those where there was a significant disc present, and those where there was, perhaps, only a tenuous disc. The distinction being approximately an order of magnitude in p . The earlier position angle determinations are consistent with that expected from the interferometry measurements made by

Table 10. The polarization of Achernar over time.

Date	p (per cent)		θ (°)	Band	Reference
31/1/1968	0.03	± 0.01	26 ± 10	V	Serkowski (1970)
12/12/1968	0.02	± 0.01	46 ± 14	V	Serkowski (1970)
1969–70 ^a	0.011	± 0.004	136.2 ± 10.4	V	Schröder (1976)
1977–78 ^a	0.001	± 0.005		400–700 nm	Tinbergen (1979)
1/9/1995 ^b	0.14	± 0.04	41 ± 8	V	McDavid (2005)
1/9/1995 ^b	0.11	± 0.05	45 ± 13	B	McDavid (2005)
7/2006 ^c	0.159	± 0.003	31.7 ± 0.6	V	Carciofi et al. (2007)
9-11/2006 ^c	0.130	± 0.001	32.6 ± 0.3	V	Carciofi et al. (2007)
9-11/2009 ^{cd}	0.011	± 0.013		B	Domiciano de Souza et al. (2014)
29/6/2011 ^d	0.016	± 0.038		B	Domiciano de Souza et al. (2014)
9-10/2011 ^{cd}	0.020	± 0.015		B	Domiciano de Souza et al. (2014)
9-11/2011 ^{cd}	0.015	± 0.009		V	Domiciano de Souza et al. (2014)
1/7/2012 ^d	0.017	± 0.015		V	Domiciano de Souza et al. (2014)
21/11/2012 ^d	0.035	± 0.050		V	Domiciano de Souza et al. (2014)
2/9/2014	0.269 84	$\pm 0.000 45$	31.5 ± 0.1	g'	This work.
24/5/2015	0.160 52	$\pm 0.000 62$	31.8 ± 0.2	g'	This work.

Notes. ^aExact dates of observations not reported.

^bMeasurements for U , R and I bands also reported in McDavid (2005) are the same within error as the B and V band measurements.

^cFor the sake of brevity, we have averaged similar measurements reported by Carciofi et al. (2007) and Domiciano de Souza et al. (2014). In the case of the former, the measurements were weighted by the number of wave-plate positions indicated. Where $p/\sigma > 4$ debiasing has been carried out as $\sqrt{p^2 - \sigma^2}$, otherwise the median is given for p , as recommended by Clarke (2010).

^dPosition angles not reported.

Domiciano de Souza et al. (2014). However, our measurements, and the averages of those made by Carciofi et al. (2007) are more precise and disagree by $\sim 5^\circ$. Carciofi et al. (2007) observed the polarization to change in both degree and angle on a time-scale of days to weeks, as well as on hour long time-scales. They interpreted the change in position angle as likely associated with a departure from a simple 2D geometry for the disc. Changes in position angle of the order of 5° , and in the degree of polarization of ~ 0.02 per cent were seen to occur on time-scales of less than an hour.

Here, our values represent observations made over a little less than half an hour each, so it is reasonable to assume we have seen a distorted disc geometry due to the addition of transitory blobs. Our measurement of 2014 September 2 represents the highest polarization ever measured for Achernar (the previous highest being that of Carciofi et al. 2007 on 2006 July 14 of 0.188 ± 0.009 per cent) and thus the greatest recorded build-up of circumstellar material. By the 2015 May 24, the polarization level had dropped by a third, but was still, historically speaking, very high.

From Table 10, our measurements are far more precise than those recorded previously. HIPPI therefore has a previously unseen capacity to probe the growth and dynamics of circumstellar discs around Be stars. The growth and dynamics of circumstellar discs are still poorly understood (Carciofi et al. 2007), high-precision polarimeters like HIPPI clearly offer an enhanced capacity to study this phenomenon.

4.9 B stars

Setting aside the Be stars, Table 6 makes it clear that B stars are more polarized than A, F, G, and K type stars. The starkness of the transition from A stars is shown up particularly well in Fig. 2; it also appears that early B stars are more polarized than later B stars. After excluding the Be stars, the close binaries and the unusual debris disc system ϵ Sgr, there are five stars of B spectral type remaining. Although the case for γ Crv and α Mus (which is 96.7 pc distant) is marginal, they all have polarizations that are higher than would be expected from only interstellar polarization when considering their positions in Figs 5 and 6.

Early-type stars can be expected to have higher magnetic fields in general as a consequence of their younger age. Some Bp (Briquet 2015) and Be stars (Hubrig et al. 2013) have been shown to have significant magnetic fields (though the fields in Be stars are weak – less than ~ 100 Gauss). However, no magnetic fields have been detected in ‘normal’ B stars within a margin of error of 13 Gauss (Shorlin et al. 2002). Consequently, we do not expect these stars to show polarization from differential saturation of Zeeman components or similar mechanisms.

One possibility to account for the high degree of polarization is that these might be debris disc host stars. Infrared excess associated with debris discs is preferentially found in young systems. However, Padgett et al. (2012) have recently, from *WISE* data, given the portion of B stars within 120 pc hosting debris discs as 12.1 ± 2.0 per cent. Similarly Schultz & Wiemer (1975) found an infrared excess – indicative of a debris disc system – in 20 of 350 O and B stars. Given that we have already identified one such system in our survey, the probability of many more is low.

A feature of B type stars is that many of them have a high rotational velocity. From Table 1, it can be seen that α Gru, β Lib and σ Sgr all have quite high rotational velocities. The spread in distances of these objects is quite large, and so we have plotted p/d against rotational velocity in Fig. 8 to attempt to reduce the effects of interstellar polarization. Fig. 8 shows B stars with higher

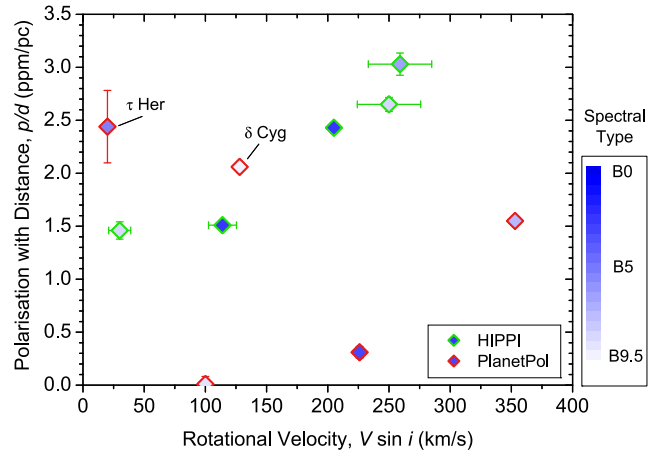


Figure 8. Polarization with distance, p/d as a function of rotational velocity for B stars without other identified polarigenic mechanisms. For the stars in our survey, there is a clear trend in increased polarization with rotational velocity, whilst for the stars in the PlanetPol survey two objects do not fit the trend: τ Her and δ Cyg. Parameters for the PlanetPol stars come from Bailey et al. (2010).

rotational velocities tend to have higher polarizations. It appears that there is an exponential increase in p/d with $V \sin i$. There are no exceptions to this trend in our data, but there are two stars surveyed by PlanetPol that do not fit.

τ Her has a high p/d , especially amongst stars from the PlanetPol survey. However, it lies at 94.6 pc distance, where we have very few stars, and the polarization of the interstellar medium is not well constrained. The degree of polarization we measured could be indicative of the edge of the Local Bubble – as originally suggested for this object by Bailey et al. (2010). So, the polarization measured could be interstellar in origin, but the lack of other objects at similar distances in the same part of the sky makes it hard to draw conclusions. The polarization of δ Cyg is not so easily explained away as being interstellar. It is a multiple system but the B component (F1V) is sufficiently separated that we would not expect this to be the polarigenic mechanism in this case. It could be that δ Cyg has a high rotational velocity, but a low inclination giving a low value for $V \sin i$, but this is purely speculation.

There are two candidates for a polarigenic mechanism related to rotational velocity. We begin by investigating that proposed by Bailey et al. (2010) for Regulus (BS 3982) – the star with the highest $V \sin i$ in Fig. 8.

4.9.1 Rotational oblateness

Based on the work of Chandrasekhar (1946) on revealing limb polarization with an eclipsing binary used to break the symmetry of the disc, Öhman (1946) reasoned that a rotationally flattened star must show polarization at all times. Detailed modelling of the expected behaviour has since quantified the effect expected, with the most recent predictions relevant to broad-band polarimetry being made by Sonneborn (1982). The magnitude of the polarization expected is now believed to be much lower than originally suggested, and in almost 70 yr of searching, polarization induced by electron scattering in a rotationally flattened atmosphere has not yet been confirmed.

A degree of polarization of 500 ppm parallel to the rotational axis is expected at 450 nm for a B0 star inclined at 90° and rotating at 95 per cent of its critical velocity. This amount is greatly reduced for

inclination angles more face on. It also decreases with increasing spectral type, with the maximum in the visual also shifting redder. The progression is dramatic with a B5 star expected to show at most 50 ppm at 700 nm (Sonneborn 1982).

As already mentioned, Bailey et al. (2010) have proposed this mechanism for the B6 star Regulus, which rotates at 86 per cent of its critical velocity (McAlister et al. 2005). Regulus is close by in a part of the sky with low interstellar polarization and registered 36.8 ± 1.6 ppm at an effective wavelength of 741.2 nm with PlanetPol. We believe Regulus still to be the best candidate for demonstrating polarization due to rotational oblateness, but unless the effect has been significantly underestimated, it cannot explain the high polarization of the other B-type stars seen here.

We see larger polarizations in g' than were seen by PlanetPol in its redder pass-band (~ 575 – 1025 nm). There is no trend with spectral type in Fig. 8, and our stars are rotating much slower than Regulus. Even accounting for a more significant interstellar contribution to the observed polarization, the excess observed is far too large to be attributed to rotational oblateness.

4.9.2 B stars as Be stars

Another possibility is that the B stars that show significant polarization are actually Be stars outside of an emission phase, or that the polarization we see is the result of a kind of sub-Be behaviour, or perhaps evidence for a polar wind in the absence of a CSE. In particular, if a small amount of ejected gas is present at the equatorial regions this could produce the observed polarization. This hypothesis is advanced on account of the rotational velocity trend (Fig. 8) as well as the sharp division between A and B type stars in the H-R diagram (Fig. 2). The statistical analysis of Yudin (2001) shows a triangular distribution for Be star polarization with $V \sin i$ that peaks at 200–250 km s⁻¹, we have far fewer B stars, but the distribution is not inconsistent with that picture. It has been suggested that faster rotators are more likely to have polar winds and as a result a circumstellar disc (Stee & Meilland 2009).

A general description of Be behaviour and the transition from B to B_{shell} to Be has already been given in Section 4.8. In early-type Be stars, the strong winds are enough to drive material away from the star creating the CSE. That the winds of B stars are weaker might be a problem for this hypothesis, but later type Be stars have weaker winds and still show Be behaviour. Other mechanisms like non-radial pulsations, magnetic activity and binarity have been advanced to explain CSE development in later Be stars (Stee & Meilland 2009; Saad et al. 2012).

It is worth keeping in mind that the levels of polarization we are seeking to explain are only ~ 100 ppm – the same level recorded by Schröder (1976) for Achernar attributed to a disc-free state. This is more than three orders of magnitude lower than the level modelled by Wood, Bjorkman & Bjorkman (1997) for the Be star η Tau for instance. Naively scaling the amount of infrared excess they modelled for their thin disc model in correspondence with the degree of polarization, we see here would result in something very difficult to detect given that infrared excess is attributable to gas and dust. Indeed from Table 1, it can be seen that the excess from B stars is not too different from that of Be stars in the survey. So, it may well be that polarization is now a more sensitive probe of close circumstellar gas than infrared excess. It is certainly more sensitive than emission line measurements, as when there is little gas there is no emission. Furthermore, polarization is more sensitive to the inner part of any disc, whereas infrared is a better probe of the

Table 11. Repeat observations of σ Sgr.

Date	p (ppm)	PA (°)
1/9/2014	175.1 ± 3.8	130.5 ± 1.3
22/5/2015	164.5 ± 5.9	129.0 ± 2.1

outer parts (Wood et al. 1997). We could be seeing a tenuous proto-CSE, and while a weak wind might not prevent a gas disc forming, it would likely prevent it developing as readily.

Recently the issue of transition from B to Be star was looked into by Barnsley & Steele (2013). They examined H α variability in a representative sample of Be stars. They formed a number of conclusions: (1) that the full phase of transition between B and Be star probably occurs over centuries, (2) that stars with earlier spectral type and higher $V \sin i$ show greater variability in H α emission, and (3) that for stars with smaller $V \sin i$ or later spectral type variability was more likely on longer (years) time-scales. What we take away from this is that stars with a higher rotational velocity or an earlier spectral type are more likely to show the emission characteristics of classical Be stars. But that any B star might become a Be star at any point in time, and that for slower later stars the behaviour is more subtle.

It stands to reason then that B stars with higher rotational velocities are also more likely to form the gas shells needed for emission behaviour, even if insufficient gas is actually stockpiled to generate the emission. If this is the case, we would expect these shells to form at equatorial latitudes and result in polarization perpendicular to the rotational axis just like in Be stars (Porter & Rivinius 2003; Saad, Hamdy & Abolazm 2012; Domiciano de Souza et al. 2014). Furthermore, whilst variations in degree of polarization are expected, variations in the polarization angle should be small – as they are with Achernar for instance. This hypothesis has the advantage of explaining the trend we see with $V \sin i$ but also allowing for the exceptions of τ Her and δ Cyg.

A pair of observations of σ Sgr (HIP 92855, B2V) shows the expected Be-like behaviour, albeit at a marginal level (Table 11). Our observations therefore represent evidence for subBe behaviour in ‘ordinary’ B stars. Incidentally, the inclination of σ Sgr has been estimated as $42 \pm 4^\circ$, putting its rotational velocity at 60–78 per cent of critical (Hutchings, Nemeč & Cassidy 1979)⁷ – in line with typical Be stars. Higher than normal X-ray emission for σ Sgr has also been seen by *XMM Newton* (Oskinova 2012), which according to Hubrig et al. (2013) is a behaviour associated with the Be phenomenon.

After σ Sgr, the next most polarized ‘ordinary’ B star in the survey is β Lib (HIP 74785, B8Vn). Notably, it has the highest infrared excess amongst these stars (Table 1). The inclination of β Lib has been estimated as 59^{+11}_{-8} (i.e. 45–64 per cent of critical velocity) by Hutchings et al. (1979). The case for β Lib being a Be star is strengthened by its listing in SIMBAD as a variable star – rare/occasional low-level photometric variability being associated with fading in late Be stars (Hubert & Floquet 1998) – if it is variable it must be so on long time-scales as it has been recommended as a photometric standard by a variety of later sources (e.g. Adelman 2001, references within Baade 1989). Additionally McLaughlin (1932b) made a rather extraordinary aside in examining plates of β Lib from 1912 to 1915 (to test a claim that it was a spectroscopic

⁷ Note the star name is incorrectly given as 6 Sgr in that work.

binary⁸), saying, ‘Only the Balmer series of hydrogen is at once evident, and these lines are so broad and diffuse that measurements are difficult, even on overexposed plates. On some spectrograms H_γ and H_δ appear triple, as if weak emission were present’.⁹

4.10 Late giants

The survey also contains a significant fraction of late-type giants. Two of these have significant previously measured polarizations: HIP 89931 (δ Sgr, K3III) at the 10^{-4} level (Tinbergen 1982) and the SRB type pulsating variable HIP 112122 (β Gru, M5III) also at the 10^{-4} level (Heiles 2000). Both of these stars also show polarizations at that level here. As discussed earlier in Section 4.1 our measurements are significantly different to the earlier ones, indicating that the polarization is variable and therefore intrinsic to the star. In addition, HIP 79593 (δ Oph) has a similarly high polarization. At 61.3 pc distance, a polarization of 131.1 ppm for HIP 110130 (α Tuc, K3III) might suggest that it is also intrinsically polarized. When one considers that in the PlanetPol survey that the M0 giants α Vul (BS 7405) and γ Sge (BS 7635) recorded 1321.4 and 199.5 ppm, respectively, this amounts to four out of eight luminosity class III M giants from the two surveys that are probably intrinsically polarized, and very probably two K type class III giants that are as well, based purely on the degree of polarization. In addition, careful examination of the spatial distribution and p/d relations in Section 4.3 suggests that γ Dra (BS 6705, K5III) and κ Lyr (BS 6872, K2III) may also belong to this group. Likewise α Phe (BS 2081, K0.5IIIb) has a polarization/distance of 3.17 ppm pc^{-1} , higher than any other star we consider to show interstellar polarization only.

From Fig. 2, we see that the degree of polarization tends to increase with spectral type and also with luminosity in these stars. Dyck & Jennings (1971) examined polarization in 55 K and M giants and supergiants. They found that almost all supergiants displayed significant polarization and that class III giants displayed an increasing likelihood of being polarized with spectral type from M3 later. However, the sensitivity of their study was no better than 10^{-3} – 10^{-4} . Given the results presented here, it now appears that many warmer giants are also intrinsically polarized, just to lower levels. Indeed, the study by Dyck & Jennings (1971) includes δ Oph, α Vul and γ Sge determining no intrinsic polarization in each case.¹⁰

Dyck & Jennings (1971) studied the wavelength dependence of the polarization in these stars, finding that it increased as λ^{-1} before tailing off at blue or violet wavelengths, where the exact peak varied from star to star. For an M0 spectral type, the effective wavelength for HIPPI is $2.094 \mu\text{m}^{-1}$ whereas for PlanetPol it was $1.264 \mu\text{m}^{-1}$. This means that HIPPI is 1.66 times as sensitive to this phenomenon as PlanetPol was. Indeed, if one applies this factor to the median polarization given for M stars by PlanetPol in Table 6, the value is closer to that obtained by our survey.

⁸ Even today it is uncertain whether β Lib is a binary – Roberts et al. (2007) have identified a second star ~ 2.1 arcsec away, but they indicate follow-up observations are needed to confirm it is not a background star. If it is a companion its spectral type is estimated as M2V.

⁹ This statement gains greater significance when one realizes that McLaughlin authored two other papers on Be star spectroscopy in the same year (Curtiss & McLaughlin 1932; McLaughlin 1932a), and was thus well practised in identifying emission characteristics in the photographic plates of the time.

¹⁰ Dyck & Jennings (1971) also measured another three stars from the PlanetPol survey without significant polarizations.

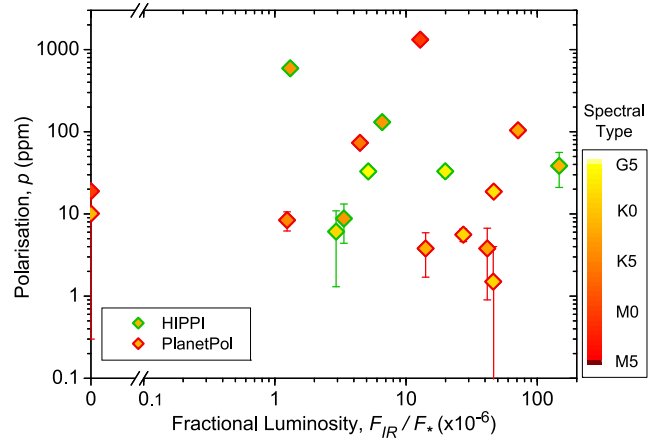


Figure 9. Polarization with infrared excess in giants later than G5. Note that HIPPI is 1.66 times as sensitive as PlanetPol at detecting polarization caused by dust in red giants, but that it also sampled a region with a higher interstellar polarization. Fractional luminosities come from McDonald et al. (2012), other parameters for the PlanetPol stars come from Bailey et al. (2010).

4.10.1 Circumstellar dust

Dyck & Jennings (1971) also noted that all the stars in their survey with significant polarizations were variable stars and that they all had an infrared excess at $11 \mu\text{m}$ (which is associated with TiO dust, TiO being one of the first molecules formed in a cooling stellar environment). Some variability was common, and was, in fact, one of the criteria used to assign polarization as intrinsic. The combination of these properties resulted in the cause of the polarization to be attributed as scattering or absorption from a circumstellar shell of solid condensates (Dyck & Jennings 1971; Jennings & Dyck 1972). In this picture, dust forms in the circumstellar environment around giant stars through a two-step process: pulsations in the outer envelope elevate molecular gas to the surface, whence the stellar wind blows it radially outwards to condense as grains in a cooler environment (Morris 1987). Dust is associated with IR excess and many red giants have significant IR excess (cf. McDonald et al. 2012). For polarization to be induced from the dust requires that the CSE be asymmetric with respect to the observer. There are a number of potential causes of the asymmetry which are debated. It has been shown that the wavelength dependence of polarization due to circumstellar dust depends on particle size and composition (McCall & Hough 1980; Raveendran 1991) as well as the geometry of the system. Silicate or carbonaceous grains are most common, however polarization may also result from scattering from inner shells of condensates able to form in hotter regions such as corundum and iron-poor silicates which are transparent at NIR wavelengths (Ireland et al. 2005).

In all, there are 24 giants, a bright giant and a supergiant later than G5 in both surveys. Of these 18 appear in the infrared excess catalogue of McDonald et al. (2012). All but two have an excess greater than 1×10^{-6} in fractional luminosity, with a range encompassing $11 \mu\text{m}$, peaking around $12 \mu\text{m}$ or shorter. We plot polarization with infrared excess in Fig. 9. This reveals that the degree of polarization is not well correlated with infrared excess. This does not necessarily mean that dust is not a prominent scatterer in the outer regions of these stars, just that the amount of dust does not account for the degree of polarization seen. Geometrical considerations may be dominant, which might indicate that the stellar winds of later giants are less symmetrical, and consequently

Table 12. Individual measurements of δ Oph.

Filter ^a	Date	q (ppm)	u (ppm)	p (ppm)	θ (°)
g'	12/5/14	-15.4 ± 6.0	-487.2 ± 4.9	487.5 ± 5.5	134.1 ± 0.7
r'	24/5/15	-44.5 ± 9.1	-391.2 ± 9.2	393.7 ± 9.1	131.8 ± 1.3
g'	24/5/15	-84.8 ± 7.2	-473.0 ± 7.1	480.6 ± 7.2	129.9 ± 0.9
425SP	24/5/15	-109.4 ± 28.3	-433.1 ± 28.2	466.7 ± 28.2	127.9 ± 3.6

Note. ^aThe effective wavelength for each filter in μm^{-1} is: 425SP: 2.502, g' : 2.094, r' : 1.654.

produce increasingly asymmetric dust-discs. In the model of Johnson & Jones (1991), an asymmetric wind develops with a star's entry on to the asymptotic giant branch (AGB). Our observations here might indicate that it occurs sooner. Alternatively, a cooler atmosphere allows dust to form closer to the photosphere, which would produce a larger polarization signal due to an increased scattering density.

4.10.2 δ Oph and other mechanisms

To investigate further, we followed up our initial 2014 May observation of the suspected variable (Percy & Shepherd 1992) δ Oph with observations made in three different wavelength bands in 2015 May. This object is particularly interesting because it features in the work of both Tsuji (2008) on MOLspheres (extended molecular spheres thought to exist beyond the photosphere) and the work of Ryde et al. (2015) which largely refutes the need for a MOLsphere to explain spectral features such as metallic emission lines, OH lines and HF lines at 12 μm . Ryde et al. (2015) claimed that all of their sample, including δ Oph, were dust free, and used this as an argument against certain absorption features being produced in the MOLsphere against a continuum formed from an alumina dust shell.

The measurements of δ Oph taken a year apart produced the same degree of polarization within the error of the measurement as shown in Table 12. However, the polarization in q was substantially different: -84.8 ± 7.2 ppm for the later measurement compared to -15.4 ± 6.0 ppm for the earlier one. The polarization of δ Oph is therefore varying, even if the large, nearly static, value for u masks the variation if just looking at the polarization degree or angle. The follow up measurements reveal behaviour consistent with dust as a scatterer, i.e. an increase as λ^{-1} between g' and r' before a less steep increase in polarization for the 425SP filter; this is shown in Fig. 10. The polarization angle in all three bands is the same within the error of the measurements.

Clarke & Schwarz (1984) and Schwarz (1986) were able to show that circumstellar dust is not the only mechanism responsible for polarization of red giants. Harrington (1969), in reference to Mira variables, was the first to propose that Rayleigh scattering from the photosphere could be responsible for the observed polarization. This mechanism was initially ruled out by Dyck & Jennings (1971) on the basis that the wavelength dependence was inconsistent with the λ^{-4} dependence of Rayleigh scattering. It was not until spectropolarimetry of supergiant Betelgeuse (α Ori) revealed polarization that changed across, and was correlated with, spectral lines of, in particular, TiO (Clarke & Schwarz 1984; Schwarz 1986), and that the λ^{-1} relationship seen was an artefact of *broad-band* polarimetry that this mechanism was accepted. This mechanism of Rayleigh or Thompson scattering from hot-spots or convection cells in the photosphere is able to explain polarization that varies regularly (in regular variables) on time-scales of months to years, whereas alternate mechanisms such as non-radial pulsations, or an equator

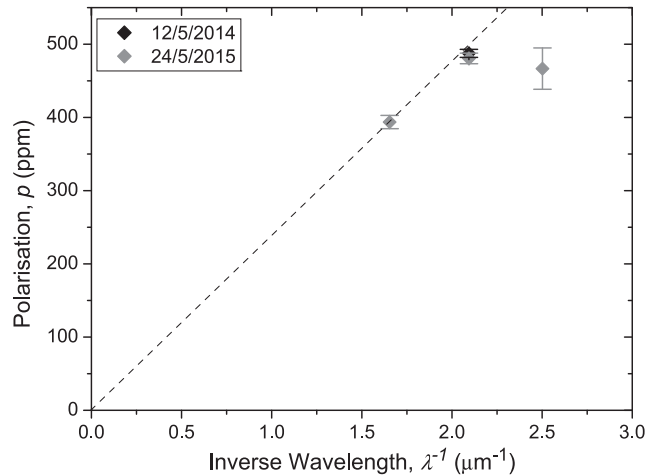


Figure 10. Polarization measurements for δ Oph with inverse wavelength. The dashed guide-line is drawn from the origin through the first data point. The second data point lies close to the guide-line, showing a λ^{-1} relationship.

to pole temperature gradient cannot (Schwarz 1986). If there are multiple hot-spots, a polarization angle that varies fairly smoothly across bands can also be expected, however that is not the case here. Hot-spots as the origin of polarization does not preclude the presence of additional scattering regions as well. In fact, changes in polarization across TiO lines point to TiO as an absorber or scatterer in the outer photosphere of highly polarized stars. It seems reasonable to expect that should hot-spots be the cause of polarization in δ Oph, then molecules like water, be they present in an extended cool photosphere or in a MOLsphere would also have spectral lines with a polarization different to the surrounding spectral continuum.

Star-spots are also a possibility, with Saar & Huovelin (1993) having calculated maximum polarizations for late giants from this mechanism of a few hundred ppm. Being evolved stars red giants are generally thought of as being inactive. However, a wavelet analysis carried out by Hedges et al. (2013) found evidence of star-spots in 14 out of a subsample of 416 red giants observed by the Kepler satellite. Very recently significant magnetic activity has been detected in Mira (Vlemmings et al. 2015), and the RS CVn K giant V* XX Tri is famous for being observed with a 'superspot' covering 11 per cent of its surface area (Künstler, Carroll & Strassmeier 2015). Hedges et al. (2013) analysis revealed features that could persist for a few hundred days. Even so, this is not the norm, and seems the most unlikely candidate for the polarization seen in δ Oph. The consistency seen in our two g' measurements a year apart would put δ Oph at the extreme end of the range with regard to the persistence of such features. The maximum polarizations calculated by Saar & Huovelin (1993) rely on a filling factor of 24 per cent, and something approaching this level would have to be present to see a ~ 500 ppm polarization. This does not fit for a star not known to be magnetically active.

Furthermore, similar degrees of polarization are calculated for g' by Leroy (1990) due to differential saturation of spectral lines in magnetic fields. Leroy (1990) was most interested in K dwarfs, but also looked at a K giant. That analysis shows that polarization due to differential saturation should be greatest in the 425SP band – which is not the case for δ Oph – a worked example spectrum for Arcturus (BS 5340, K1.5III) with a hypothetical 500 Gauss field is shown. Arcturus was observed as part of the PlanetPol survey, recording 6.3 ± 1.6 ppm; whereas in PlanetPol's waveband the calculation yields around 150 ppm. If this mechanism were primarily responsible for the polarization we see in M and K giants, we might expect the ratio of median polarizations determined by HIPPI and PlanetPol to be similar for M and K spectral types, which is not what we see in Table 6.

5 CONCLUSIONS

50 of the brightest stars in the Southern hemisphere have been observed for their linear polarization. We have investigated these alongside 49 Northern stars from the PlanetPol survey. These two surveys are far more sensitive than previous stellar polarimetric surveys. Prior to this work, aside from the four classical Be stars, none of the stars had identified intrinsic polarization assigned to them. We have now attributed polarigenic mechanisms to around half of the stars in the survey. In particular, B type stars have been identified as being polarized through a variety of mechanisms, whilst late giants also show a greater propensity to be intrinsically polarized than demonstrated in previous studies, mostly as a consequence of circumstellar dust. Intrinsic polarization was also identified in an Ap star and in debris disc systems.

Amongst the intrinsically polarized B stars was the close binary system Spica, which demonstrated variability from repeat measurements. Of the four Be stars observed, three have been resolved by interferometry. For each of these, we measured a polarization angle aligned perpendicular to the rotational axis. We recorded the highest degree of polarization on record for the Be star Achernar in 2014 September; this indicates it was particularly active at this time. It has since declined in polarization. Other B type stars were also found to possess high levels of polarization. Since most of the B stars rotate at well below break-up velocity, (Regulus in the PlanetPol survey being an exception) this cannot be a result of rotational oblateness. Instead, we advance the hypothesis that what we are observing is low level Be-like behaviour in normal B stars.

There are only a small number of debris disc systems in the combined catalogue of the two surveys, but these show a slight tendency to be more polarized than other nearby stars. The circumbinary debris disc system ϵ Sgr appears to have a polarization signature consistent with a companion-induced asymmetry in light scattered from the disc.

Many of the M and K giants in the surveys are clearly intrinsically polarized with cooler and more luminous stars having higher polarizations. Infrared excess is not correlated with the degree of polarization in our sample. However circumstellar dust distributed by an asymmetric stellar wind may be responsible for the trends we see. Increased scattering density from dust closer to the photosphere in cooler stars might also be responsible for the trend. However, the dust free M giant δ Oph also displays a variable and high degree of polarization. This behaviour may be associated with Rayleigh scattering from stellar hot-spots, or less likely star-spots.

The plethora of polarized stars identified has profound consequences for polarimetric studies of the local interstellar medium, and for searching out other polarimetric effects nearby. It is

common practice to determine a value for the interstellar polarization of an object thought to have some interesting intrinsic effect by taking an average of the measured polarizations of nearby stars. Stars are selected for this purpose on the basis that they are likely to be unpolarized. Our study shows that if one seeks a value for the interstellar polarization at the ppm level then, in particular, no B type stars nor M or K giants should be selected. Ap stars and debris disc systems should also be avoided. As these are some of the brightest stars at any given distance and otherwise likely to be selected this is an important finding.

When we discount the intrinsically polarized stars from our sample and that of the PlanetPol survey, we find that interstellar polarization is stronger in Southern stars. Away from the Galactic equator in the Northern sky stars are polarized at $\sim 2 \times 10^{-7}$ pc $^{-1}$. At distances between 10 and 30 pc in the Southern sky, the rate of polarization can be as much as $\sim 2 \times 10^{-6}$ pc $^{-1}$. Beyond 30 pc there appears to be less of a polarizing effect from the interstellar medium. The polarization angles of stars just to the Galactic north are aligned to the Galactic equator. A dustier interstellar medium to the south (in the direction of the centre of the galactic plane) appears primarily responsible for the higher degrees of interstellar polarization observed in Southern stars within 100 pc.

The very high precision of HIPPI in fractional polarization has allowed us to uncover the polarimetric behaviour of some of the best known stars in the night sky. We have demonstrated HIPPI's potential in many areas of stellar polarimetry, producing more precise measurements than have previously been possible and indeed uncovering the polarigenic behaviour of some stars previously searched for but not found. HIPPI's simplicity and economical fabrication belies its great value.

ACKNOWLEDGEMENTS

The development of HIPPI was funded by the Australian Research Council through Discovery Projects grant DP140100121 and by the UNSW Faculty of Science through its Faculty Research Grants programme. The authors thank the Director and staff of the Australian Astronomical Observatory for their advice and support with interfacing HIPPI to the AAT and during our observing runs on the telescope. We acknowledge the use of the SIMBAD database and this research has made use of the VizieR Service at Centre de Données Astronomiques de Strasbourg.

REFERENCES

- Absil O. et al., 2013, *A&A*, 555, A104
- Abt H. A., Levato H., Grosso M., 2002, *ApJ*, 573, 359
- Adelman S. J., 2001, *A&A*, 367, 297
- Baade D., 1989, *A&AS*, 79, 423
- Bailey J., 2007, *Astrobiology*, 7, 320
- Bailey J., Lucas P. W., Hough J. H., 2010, *MNRAS*, 405, 2570
- Bailey J., Kedziora-Chudczer L., Cotton D. V., Bott K., Hough J. H., Lucas P. W., 2015, *MNRAS*, 449, 3064
- Barnsley R. M., Steele I. A., 2013, *A&A*, 556, A81
- Bartkevicius A., Gudas A., 2001, *Balt. Astron.*, 10, 481
- Behr A., 1959, PhD thesis, Univ. Gottingen
- Briquet M., 2015, Magnetic fields in O-, B- and A-type stars on the main sequence. EPJ Web of Conf. 101, EDP Sciences, 05001
- Burnham R, Jr, 1978a, *Burnham's Celestial Handbook: Volume One, Andromeda through Cetus*. Dover Press, New York
- Burnham R, Jr, 1978b, *Burnham's Celestial Handbook: Volume Two, Chamaeleon through Orion*. Dover Press, New York

- Burnham R. Jr, 1978c, *Burnham's Celestial Handbook: Volume Three*, Pavo through Vulpecula. Dover Press, New York
- Carciofi A. C., Magalhães A. M., Leister N. V., Bjorkman J. E., Levenhagen R. S., 2007, *ApJ*, 671, L49
- Carciofi A. C., Bjorkman J. E., Otero S. A., Okazaki A. T., Štefl S., Rivinius T., Baade D., Haubois X., 2012, *ApJ*, 744, L15
- Castelli F., Kurucz R. L., 2004, in Piskunov N. et al., eds, *Proc. IAU Symp.* 210, *Modelling of Stellar Atmospheres*.
- Chandrasekhar S., 1946, *ApJ*, 103, 351
- Chen C. H., Mittal T., Kuchner M., Forrest W. J., Lisse C. M., Manoj P., Sargent B. A., Watson D. M., 2014, *ApJS*, 211, 25
- Clarke D., 2010, *Stellar Polarimetry*. Wiley, New York
- Clarke D., Schwarz H. E., 1984, *A&A*, 132, 375
- Cummings I. N., 1998, PhD thesis, Univ. Canterbury
- Curtiss R. H., McLaughlin D. B., 1932, *Publ. Michigan Obs.*, 4, 163
- de Medeiros J. R., Mayor M., 1999, *A&AS*, 139, 433
- De Medeiros J. R., Alves S., Udry S., Andersen J., Nordström B., Mayor M., 2014, *A&A*, 561, A126
- Díaz C. G., González J. F., Levato H., Grosso M., 2011, *A&A*, 531, A143
- Domiciano de Souza A., Kervella P., Jankov S., Abe L., Vakili F., di Folco E., Paresce F., 2003, *A&A*, 407, L47
- Domiciano de Souza A. et al., 2014, *A&A*, 569, A10
- Dring A. R., Murthy J., Henry R. C., Walker H. J., 1996, *ApJ*, 457, 764
- Dyck H. M., Jennings M. C., 1971, *AJ*, 76, 431
- Eggleton P. P., Tokovinin A. A., 2008, *MNRAS*, 389, 869
- Eiroa C. et al., 2013, *A&A*, 555, A11
- García L., Gómez M., 2015, *Rev. Mex. Astron. Astrofis.*, 51, 3
- Głębocki R., Gnaniński P., 2005, in Favata F., Hussain G. A. J., Battrick B., eds, *ESA SP-560: 13th Cambridge Workshop on Cool Stars, Stellar Systems and the Sun*. ESA, Noordwijk, p. 571
- Harrington J. P., 1969, *Astrophys. Lett.*, 3, 165
- Harrington D., Koenigsberger G., Moreno E., Kuhn J., 2009, *ApJ*, 704, 813
- Hayes D. P., 1984, *AJ*, 89, 1219
- Hayes D. P., 1986, *ApJ*, 302, 403
- Hedges C., Mathur S., Thompson M. J., MacGregor K. B., 2013, in Shibahashi H., Lynas-Gray A. E., eds, *ASP Conf. Ser. Vol. 479, Progress in Physics of the Sun and Stars: A New Era in Helio- and Asteroseismology*. Astron. Soc. Pac., San Francisco, p. 197
- Heiles C., 1996, in Roberge W. G., Whittet D. C. B., eds, *ASP Conf. Ser. Vol. 97, Polarimetry of the Interstellar Medium*. Astron. Soc. Pac., San Francisco, p. 457
- Heiles C., 2000, *AJ*, 119, 923
- Hough J. H., Lucas P. W., Bailey J. A., Tamura M., Hirst E., Harrison D., Bartholomew-Biggs M., 2006, *PASP*, 118, 1302
- Hubert A. M., Floquet M., 1998, *A&A*, 335, 565
- Hubrig S., Le Mignant D., North P., Krautter J., 2001, *A&A*, 372, 152
- Hubrig S., Schöller M., Ilyin I., González J. F., Mikulášek Z., 2013, *Cent. Eur. Astrophys. Bull.*, 37, 155
- Hutchings J. B., Nemeč J. M., Cassidy J., 1979, *PASP*, 91, 313
- Ireland M. J., Tuthill P. G., Davis J., Tango W., 2005, *MNRAS*, 361, 337
- Jennings M. C., Dyck H. M., 1972, *ApJ*, 177, 427
- Johnson J. J., Jones T. J., 1991, *AJ*, 101, 1735
- Joshi Y. C., 2007, *MNRAS*, 378, 768
- Keller C. U., 2006, in McLean I. S., Iye M., eds, *Proc. SPIE Conf. Ser. Vol. 6269, Ground-based and Airborne Instrumentation for Astronomy*. SPIE, Bellingham, art id. 62690
- Kemp J. C., Karitskaya E. A., Kumsiashvili M. I., Lyutij V. M., Kruzina T. S., Cherepashchuk A. M., 1987, *Astron. Zh.*, 64, 326
- Kim S.-H., Martin P. G., Hendry P. D., 1994, *ApJ*, 422, 164
- Kochukhov O., Wade G. A., 2010, *A&A*, 513, A13
- Kopparla P., Natraj V., Yung Y. L., 2014, in *AAS/Division for Planetary Sciences Meeting Abstracts*, Vol. 46, p. 10109
- Kostogryz N. M., Berdyugina S. V., 2015, *A&A*, 575, A89
- Kostogryz N. M., Berdyugina S. V., Yakobchuk T. M., 2015, in van Belle G. T., Harris H. C., eds, *Cambridge Workshop on Cool Stars, Stellar Systems, and the Sun*, Vol. 18. Lowell Observatory, p. 773
- Künstler A., Carroll T. A., Strassmeier K. G., 2015, *A&A*, 578, A101
- Leroy J. L., 1990, *A&A*, 237, 237
- Leroy J. L., 1993a, *A&AS*, 101, 551
- Leroy J. L., 1993b, *A&A*, 274, 203
- Leroy J. L., 1999, *A&A*, 346, 955
- Lucas P. W., Hough J. H., Bailey J. A., 2006, in Arnold L., Bouchy F., Moutou C., eds, *Tenth Anniversary of 51 Peg-b: Status of and Prospects for Hot Jupiter Studies*. Frontier Group, p. 334
- Lucas P. W., Hough J. H., Bailey J. A., Tamura M., Hirst E., Harrison D., 2009, *MNRAS*, 393, 229
- McAlister H. A. et al., 2005, *ApJ*, 628, 439
- McCall A., Hough J. H., 1980, *A&AS*, 42, 141
- McDavid D., 2005, in Ignace R., Gayley K. G., eds, *ASP Conf. Ser. Vol. 337, The Nature and Evolution of Disks Around Hot Stars*. Astron. Soc. Pac., San Francisco, p. 265
- McDonald I., Zijlstra A. A., Boyer M. L., 2012, *MNRAS*, 427, 343
- McLaughlin D. B., 1932a, *Publ. Michigan Obs.*, 4, 175
- McLaughlin D. B., 1932b, *Publ. Michigan Obs.*, 4, 29
- McLean I. S., 1980, in Plavec M. J., Popper D. M., Ulrich R. K., eds, *Proc. IAU Symp. 88, Close Binary Stars: Observations and Interpretation*. Reidel, Dordrecht, p. 65
- Mallik S. V., Parthasarathy M., Pati A. K., 2003, *A&A*, 409, 251
- Massarotti A., Latham D. W., Stefanik R. P., Fogel J., 2008, *AJ*, 135, 209
- Matthews B. C., Krivov A. V., Wyatt M. C., Bryden G., Eiroa C., 2014, in Beuther H., Klessen R. S., Dullemond C. P., Henning T., eds, *Protostars and Planets VI*. Univ. Arizona Press, Tuscan, AZ, p. 521
- Meilland A. et al., 2007, *A&A*, 464, 59
- Meilland A., Millour F., Kanaan S., Stee P., Petrov R., Hofmann K.-H., Natta A., Perraut K., 2012, *A&A*, 538, A110
- Mittal T., Chen C. H., Jang-Condell H., Manoj P., Sargent B. A., Watson D. M., Lisse C. M., 2015, *ApJ*, 798, 87
- Morales F. Y., Rieke G. H., Werner M. W., Bryden G., Stapelfeldt K. R., Su K. Y. L., 2011, *ApJ*, 730, L29
- Morris M., 1987, *PASP*, 99, 1115
- Öhman Y., 1946, *ApJ*, 104, 460
- Oskimova L., 2012, *What is Nunki? XMM-Newton Proposal*
- Oudmajer R. D. et al., 2001, *A&A*, 379, 564
- Padgett D., Stapelfeldt K. R., Liu W., Leisawitz D. T., Fajardo-Acosta S., 2012, in Augereau J.-C., ed., *Herschel Observations of Debris Discs from WISE, from Atoms to Pebbles: Herschel's View of Star and Planet Formation*. Grenoble, France, p. 23
- Percy J. R., Shepherd C. W., 1992, *Inf. Bull. Var. Stars*, 3792, 1
- Perryman M. A. C. et al., 1997, *A&A*, 323, L49
- Peters G. J., 1986, *ApJ*, 301, L61
- Pfeiffer R. J., Koch R. H., 1977, *PASP*, 89, 147
- Pilbratt G. L. et al., 2010, *A&A*, 518, L1
- Poglitsch A. et al., 2010, *A&A*, 518, L2
- Porter J. M., Rivinius T., 2003, *PASP*, 115, 1153
- Pourbaix D. et al., 2002, *A&A*, 386, 280
- Pourbaix D. et al., 2004, *A&A*, 424, 727
- Raveendran A. V., 1991, *A&A*, 243, 445
- Rhee J. H., Song I., Zuckerman B., McElwain M., 2007, *ApJ*, 660, 1556
- Roberts L. C., Jr, Turner N. H., ten Brummelaar T. A., 2007, *AJ*, 133, 545
- Rodigas T. J., Follette K. B., Weinberger A., Close L., Hines D. C., 2014, *ApJ*, 791, L37
- Rodríguez D. R., Zuckerman B., 2012, *ApJ*, 745, 147
- Royer F., Gerbaldi M., Faraggiana R., Gómez A. E., 2002, *A&A*, 381, 105
- Ryde N., Lambert J., Farzone M., Richter M. J., Josselin E., Harper G. M., Eriksson K., Greathouse T. K., 2015, *A&A*, 573, A28
- Saad S. M., Hamdy M. A. H., Abolazm M. S., 2012, *NRIAG J. Astron. Geophys.*, 1, 97
- Saar S. H., Huovelin J., 1993, *ApJ*, 404, 739
- Schmid H. M. et al., 2005, in Adamson A., Aspin C., Davis C., Fujiyoshi T., eds, *ASP Conf. Ser. Vol. 343, Astronomical Polarimetry: Current Status and Future Directions*. Astron. Soc. Pac., San Francisco, p. 89
- Schneider G. et al., 2014, *AJ*, 148, 59
- Schröder R., 1976, *A&AS*, 23, 125
- Schultz G. V., Wiemer W., 1975, *A&A*, 43, 133
- Schwarz H. E., 1986, *Vistas Astron.*, 29, 253
- Seager S., Whitney B. A., Sasselov D. D., 2000, *ApJ*, 540, 504

- Serkowski K., 1970, *ApJ*, 160, 1083
- Serkowski K., 1973, in Greenberg J. M., van de Hulst H. C., eds, *Proc. IAU Symp. 52, Interstellar Dust and Related Topics*. Reidel, Dordrecht, p. 145
- Serkowski K., Mathewson D. S., Ford V. L., 1975, *ApJ*, 196, 261
- Shorlin S. L. S., Wade G. A., Donati J.-F., Landstreet J. D., Petit P., Sigut T. A. A., Strasser S., 2002, *A&A*, 392, 637
- Sokolov N. A., 2008, *MNRAS*, 385, L1
- Sonneborn G., 1982, in Jaschek M., Groth H.-G., eds, *Proc. IAU Symp. Vol. 98, Be Stars*. Reidel, Dordrecht, p. 493
- Stee P., Meilland A., 2009, *Lecture Notes in Physics*, Vol. 765, *The Rotation of Sun and Stars*. Springer-Verlag, Berlin, p. 195
- Strassmeier K. G., 2009, *A&AR*, 17, 251
- Su K. Y. L. et al., 2013, *ApJ*, 763, 118
- Thureau N. D. et al., 2014, *MNRAS*, 445, 2558
- Tinbergen J., 1979, *A&AS*, 35, 325
- Tinbergen J., 1982, *A&A*, 105, 53
- Tsuji T., 2008, *A&A*, 489, 1271
- van Belle G. T., 2012, *A&AR*, 20, 51
- van Leeuwen F., 2007, *A&A*, 474, 653
- Vlemmings W. H. T., Ramstedt S., O’Gorman E., Humphreys E. M. L., Wittkowski M., Baudry A., Karovska M., 2015, *A&A*, 577, L4
- Weise P., Launhardt R., Setiawan J., Henning T., 2010, *A&A*, 517, A88
- Wenger M. et al., 2000, *A&AS*, 143, 9
- Whittet D. C. B., Martin P. G., Hough J. H., Rouse M. F., Bailey J. A., Axon D. J., 1992, *ApJ*, 386, 562
- Wiktorowicz S. J., 2009, *ApJ*, 696, 1116
- Wiktorowicz S. J., Matthews K., 2008, *PASP*, 120, 1282
- Wiktorowicz S. J., Nofi L. A., 2015, *ApJ*, 800, L1
- Wilking B. A., Lebofsky M. J., Rieke G. H., 1982, *AJ*, 87, 695
- Wolff S. C., Strom S. E., Dror D., Venn K., 2007, *AJ*, 133, 1092
- Wood K., Bjorkman K. S., Bjorkman J. E., 1997, *ApJ*, 477, 926
- Wyatt M. C., 2008, *ARA&A*, 46, 339
- Yudin R. V., 2001, *A&A*, 368, 912
- Zamanov R. K., Bode M. F., Melo C. H. F., Stateva I. K., Bachev R., Gomboc A., Konstantinova-Antova R., Stoyanov K. A., 2008, *MNRAS*, 390, 377
- Zorec J., Royer F., 2012, *A&A*, 537, A120

This paper has been typeset from a $\text{\TeX}/\text{\LaTeX}$ file prepared by the author.